

Treball Final de Grau

Fluid circulation simulation in heat exchanger pipes of double tube: from cylindrical smooth surface to finned tubes.

Simulación de la circulación de fluidos en tuberías de intercambiadores de calor de doble tubo: de los tubos cilíndricos lisos a los aleteados.

Jesús Martín García

June 2016



**UNIVERSITAT DE
BARCELONA**

Aquesta obra està subjecta a la llicència de:
Reconeixement–NoComercial–SenseObraDerivada



<http://creativecommons.org/licenses/by-nc-nd/3.0/es/>

*L'ignorance affirme ou nie catégoriquement;
La science doute.*

François-Marie Arouet

En primer lugar quiero dedicar estas primeras líneas a las dos personas más importantes de mi vida; mis padres. Estoy seguro de que sin ellos, sin su implicación, entusiasmo y apoyo incondicional, jamás hubiese sido la persona que soy hoy en día. Han sido, son y serán, dos pilares fundamentales para mí.

En segundo lugar agradecer el apoyo de mis tutores, quienes me han ayudado a reflejar sobre estas líneas mis conocimientos, mis ideas y mi forma de ver las cosas. Desde el día que empecé el proyecto, hasta el último, han presentado una disponibilidad absoluta, abiertos siempre a hablar y a ayudarme en el avance del mismo. Quiero también dar las gracias a todos y cada uno de los profesores que he tenido a lo largo de mi vida como estudiante, pues de todos ellos me he llevado cosas positivas. Agradecer también, por supuesto, el apoyo de mis compañeros de universidad y, en definitiva, de fatigas.

Me llevo experiencias de todo tipo en esta etapa, pero, sobre todo, experiencias de vida.

REPORT

CONTENTS

1. SUMMARY	3
2. RESUMEN	5
3. INTRODUCTION	7
3.1. CFD Analysis	8
3.2. Double pipe heat exchanger	10
4. OBJECTIVES	13
5. MATERIAL, METHODS AND COMPUTATIONAL STUDY	14
5.1. Material	14
5.2. CFD Procedure	14
5.2.1. PRE-PROCESSING	15
5.2.1.1. Geometry	15
5.2.1.2. Mesh	18
5.2.2. SOLVER	20
5.2.2.1. Solver algorithms	21
5.2.2.2. Models	21
5.2.2.3. Boundary Conditions	21
5.2.2.4. Solution method	22
5.3. Computational study	23
5.3.1. GOVERNING EQUATIONS	23
5.3.2. THE ANALYSIS DOMAIN	24
5.3.2.1. Details double pipe heat exchanger	24
5.3.2.2. Details double pipe heat exchanger with fins	25

5.3.3. NUMERICAL MODELING	26
5.3.3.1. Heat transfer coefficient calculation of simulation	26
5.3.3.2. Double pipe correlations used for validation	27
5.3.3.3. Correlations for double pipe with fins used for validation	28
5.3.4. NUMERICAL METHODOLOGY	30
5.3.4.1. Design Modeler	30
5.3.4.2. Mesh	32
5.3.4.3. Solver	36
6. RESULTS AND DISCUSSION	39
6.1. Double pipe heat exchanger	39
6.1.1. Geometry	39
6.1.2. Mesh	40
6.1.3. Simulation results of the influence of heat exchanger length	41
6.2. Double pipe heat exchanger with fins	48
6.2.1. Geometry	48
6.2.2. Mesh	49
6.2.2.1. Meshing double pipe with fins	49
6.2.2.2. Improved meshing double smooth pipe	52
6.2.3. Simulation results of the influence of flow rate and presence of fins	52
7. CONCLUSIONS	60
8. REFERENCES	61
9. ACRONYMS	63

1. SUMMARY

Nowadays, and increasingly common, numerical methods using computers are setting up, both industry and teaching, to solve problems in the field of chemical engineering. The classical resolution of these problems was subject to empirical expressions adjusting the available data with a simple model that can be easily solved, said colloquially, “pencil and paper”. The resolution of the problems based on the microscopic balances of mass, energy and momentum without computer implies high computation time and inherent human mistakes. Society evolves and progresses and the technology too. The use of computers is too globalized and this is something unavoidable, so it is interesting to take advantage of this technological advance, and the increased power of these machines, to resolve microscopic balances much more quickly and accurately. There is a branch of fluid mechanics, Computational Fluid Dynamics (CFD), capable of using numerical methods and algorithms to solve and analyse problems related to fluid flow. The use of these CFD methods allows simulating the behaviour of fluid media. As the mass and energy conservation balances must be fulfilled and there are good models based on empirical data that takes into account the energy lost in the momentum balances, hence quite reliable results are obtained by CFD. CFD, therefore, presents an opportunity to have a “virtual laboratory”, where it is possible to study, simulate and obtain solutions that provide insights and better understanding of the unit behaviour. A “virtual laboratory” in all its entirety, where to test and simulate aspects that otherwise based only on experiments would require more time and resources. This project shows that the CFD tools widely used in other engineering fields such as the aeronautics is also useful for the chemical engineering purposes.

This project, taking advantage of continuous research and incorporation of software in the engineering world, gives small touches of these aspects using the simulation program ANSYS®, used to resolve microscopic balances of mass, energy and momentum, focusing on the fluid flow through pipe heat exchanger: from double pipe to another complex geometry such as finned tubes. The analysis of all possibilities raised allow to obtain a general understanding of the unit.

The results obtained provide an overview of the differences between units, helping the understanding of how the fluid behaves inside them. A comparison between the simulations results and the classical equation results is also provided.

Keywords: Heat transfer augmentation techniques, Double pipe, CFD.

2. RESUMEN

Hoy en día, y cada vez de forma más habitual, se están instaurando, tanto en la industria como en la docencia, la utilización de métodos numéricos mediante el uso de ordenadores para la resolución de problemas en el ámbito de la ingeniería química. La resolución clásica de estos problemas estaba sujeta a expresiones empíricas ajustadas a los datos experimentales disponibles de un modelo simple que podía ser resuelto fácilmente, dicho coloquialmente, "lápiz y papel". La resolución de estos problemas basados en balances microscópicos de masa, energía y cantidad de movimiento sin el uso de ordenadores implica tiempos de cálculo muy elevados y errores inherentes del ser humano. La sociedad evoluciona y progresa y con ella la tecnología. El uso de los ordenadores es un fenómeno de masas y esto es algo ineludible, así que resulta interesante aprovechar ese avance tecnológico, y el aumento en la potencia de estas máquinas, para resolver balances microscópicos de forma mucho más rápida y precisa. Existe una rama de la mecánica de fluidos, Computational Fluid Dynamics (CFD), encargada de utilizar métodos numéricos y algoritmos para resolver y analizar problemas relacionados con el flujo de fluidos. El uso de estos métodos CFD permitirá simular el comportamiento del medio fluido. Las ecuaciones de conservación de masa y energía deben cumplirse y existen buenos modelos basados en datos empíricos que tienen en cuenta la energía perdida de estos balances, por lo que mediante CFD se pueden obtener resultados bastante fiables. CFD, por tanto, nos presenta la oportunidad de disponer de un "laboratorio virtual", donde poder estudiar, simular y obtener soluciones que nos ayuden a comprender el comportamiento de la unidad. Un "laboratorio virtual" en toda su extensión, donde hacer pruebas y simular aspectos que, de otra manera, al basarse en datos experimentales, requerirían de mucho tiempo y recursos. Este proyecto muestra que las herramientas CFD son ampliamente utilizadas en otros campos de la ingeniería como pueden ser la aeronáutica y, especialmente útil, en la ingeniería química.

El proyecto que presento, aprovechando la continua investigación e incorporación de software en el mundo ingenieril, da pequeñas pinceladas de estos aspectos haciendo uso del programa de simulación ANSYS®, utilizado para resolver balances microscópicos de materia,

energía y cantidad de movimiento, centrándome en la circulación de fluidos a través de las tuberías de un intercambiador de calor: desde un doble tubo clásico a otros con formas geométricas más complejas como los tubos aleteados. El análisis de todas las posibilidades que se plantean permite obtener un conocimiento general de la unidad. Los resultados obtenidos proporcionan una visión general de las diferencias que existen entre las diferentes unidades, ayudando a entender cómo se comporta el fluido dentro de éstas. Además, se proporciona una comparativa entre los resultados de la simulación y los resultados de las ecuaciones clásicas.

Palabras clave: Técnicas de aumento de transferencia de calor, Doble tubo, CFD.

3. INTRODUCTION

In the last decade there has been a rapid development of Computation Fluid Dynamics (CFD), a result, in great measure, of the conjugate progress in numerical analysis, computer technology and visualization tools. These aspects have made possible that multiple branches of science devote their efforts to go forward and progress in this field. Nowadays, numerical methods play an important role in all branches of fundamental and applied mechanics in both research and industry.

At this time it is easy to raise the question of, which are the advantages of using CFD simulations before performing a study at laboratory scale? This question is discussed in this introduction.

First of all, the simulation is not a unit model itself, seeing that a model represents a physical reality for a specific unit operation. The simulation is rather an “imitation” of that reality from the point of view that its model based on microscopic balances is the same for any unit operation. Through this point of view then it is possible to predict the system behavior under different circumstances and configurations, even when there is not experimental data available because never before the system have been subjected to those conditions or configurations. Once the model has been built, it can be studied under different conditions, analyzing how these changes affect to the unit. Therefore, the simulation is used to improve a real system without interfering manually, without touching it. This is a very powerful tool, with freedom for exploring, studying and designing configurations for a first insight but without the costs of building the unit. The simulation often is able to solve novel unit configurations when a classical model to be solved analytically is not available. Numerical methods allow the visualization of the unit internals and achieve a deeper understanding of the process behavior than using classical equations that only focus in input and output variables. Some of the CFD results have been contrasted with real world experimental data. All these experiments provide results useful to optimize costs and time, hence the user focuses on the study and evaluation of the design of the best alternative systems from the multiples choices.

The aim of the present study is focused on the CFD simulation of a heat exchanger. A heat exchanger is a unit where heat transfer (essential part of most chemical processes) takes place. The key element of any exchanger is the tube wall where the heat is transferred but keeping separate fluids. During the design phase, the designer makes choices and performs data mining of input data: location of fluid circulation, flow direction, fluid velocity, temperature, pressure drop allowed, etc, but the main parameter is the heat flow per unit area, ensuring that the heat transfer is maximized. High velocity implies high heat transfer coefficients, but also high pressure drop. Temperatures are also very important in the design of heat exchangers as they provide the driving force. Small driving force implies large areas needed for heat transfer. Considering all these possibilities and evaluating the performance of each one experimentally involves a lot of time and cost. This is not the case when performing a simulation, as it is cheaper to try it virtually. Literature provides several important handbooks (Sinnott and Towler, 2012) where reliable design tools are found. The heat exchanger simulation provides information about the efficiency of alternative designs. Additionally, due to the computing power increase, the simulation software provides detailed information (graphical or numerical) that otherwise would be inaccessible even when the unit is physically available. To achieve this goal, the discretization (Peyret, 1996) is used, which divides the unit in a large number of small portions, analyzing the behavior of each zone.

Finally, the CFD simulations are an effective means for teaching or demonstrating concepts, which helps the student to acquire knowledge of fluid dynamics, especially its use in engineering education. Most simulators have animations, in which the dynamic of the system is visualized, providing a meaningful understanding of the system's nature together with many other tools of graphical representation.

3.1. CFD ANALYSIS

Fluid flow (liquid and gas) encountered in everyday life include: meteorological phenomena, environmental hazards heating system, combustion in automobile engines and other propulsion systems, complex flows in heat exchangers and chemical reactors, processes in human body, etc. These are governed by partial differential equations (PDE) which represent conservation laws for the mass, momentum and energy.

Computational Fluid Dynamics (CFD) is a branch of fluid mechanics that uses numerical analysis and algorithms to solve and analyze problems that involve fluid flows, replacing such PDE systems by a set of algebraic equations which are solved using digital computers. Exact

solutions for differential equations, however, are generally difficult to obtain. Numerical methods are adopted to solve the differential equations. Among these numerical methods, those which approximate continua with infinite degree of freedom by a discrete body with finite degree of freedom are called “discrete analysis”. Via these methods of discrete analysis, differential equations are reduced to simultaneous linear algebraic equations and thus can be solved numerically. More descriptions about CFD are available in the literature (Ferziger and Peric, 1996; Peyret and Taylor, 1983).

CFD analysis provides a qualitative (and sometimes even quantitative) prediction of fluids flows by means of:

- Mathematical modeling (partial differential equations).
- Numerical methods (discretization and solution techniques).
- Software tools (solvers, pre- and post-processing utilities).

This enables the user to perform numerical experiments in a “virtual flow laboratory”. Some examples of CFD applications are available in the field of aerodynamics (Figure 1) and chemical engineering.

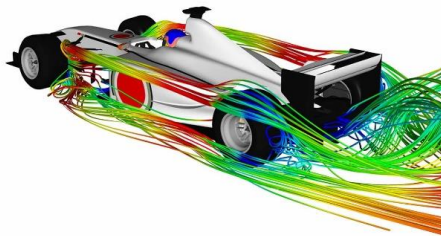


Figure 1. Aerodynamic shape design

3.2. DOUBLE PIPE HEAT EXCHANGER

A double pipe heat exchanger consists of two concentric pipes in which two fluids flow through the exchanger (when two streams flow in the same direction is called parallel flow, or counter flow when the fluids flow in opposite directions). A heat exchanger utilizes the fact that, where ever there is a temperature difference, flow of energy occurs. The flows have temperature difference and thus the driving force for the energy to flow between them. The fluid which is fed at a higher temperature than at its output is known as hot fluid. While the fluid which receives energy is known as cold fluid. Temperature of hot fluid decreases while the temperature of cold fluid increases along the heat exchanger. Accordingly, the purpose of heat exchanger is either to heat or cool a fluid. The outer annular pipe may be insulated to minimize heat transfer to the environment. This type of heat exchanger composed of two concentric tubes is really economic. Double pipe exchangers are commonly used in applications involving relatively low flow rates and high temperatures or pressures, for which they are well suited. Other advantages include low installation cost, ease of maintenance, and flexibility. Besides, heat exchangers are used in variety of applications. Some of the applications of heat exchangers are in process industries, thermal power plants, air-conditioning equipment, refrigerators, radiators for space vehicles, etc.

Heat transfer is an important discipline in chemical engineering for an efficient use of energy. An example is found in fluid mechanics, which is able to describe the heat transport clearly and precisely due to the progress made in modern heat transfer convection. In this decade, the simulation programs as ANSYS® have been mostly used for aeronautical purpose in order to define the movement of air along the planes and trying to improve the aerodynamics of the designs, also they explain thermodynamic phenomena due to modeling, simulation and energy optimization of virtual systems. These computer programs are used to optimize the architecture studied to fit into finite volumes, using change in geometry and contact surface in order to improve the heat transfer. The effective utilization of available energy is crucial to be competitive and environmentally friendly. Increase in heat exchanger performance or more economical designs improve energy recovery and material and cost savings. The need to increase the thermal performance of heat exchangers lead to the development and use of many techniques called "Heat transfer augmentation" (Bejan and Kraus, 2003). Heat transfer augmentation techniques refer to different methods used to increase the rate of heat transfer without affecting too much the overall performance of the system. These techniques are broadly divided in two groups: passive

and active. Active techniques require some power, such as electric or acoustic fields and surface vibration, whereas, passive techniques do not require any type of external power for the heat transfer augmentation. Passive heat transfer augmentation methods used generally are: coating of the surface, rough surfaces, extended surfaces, displaced inserts, swirl flow devices, etc. Nowadays, computer systems are used to advance in the study of complex geometries providing the heat transfer and pressure drop along the heat exchanger. The design of these units is a hot issue in chemical engineering. For example, Naphon (2006) investigated experimentally the flow of hot and chilled water in horizontal copper double tube heat exchanger fitted with aluminum twisted tape inside. The effects of relevant parameters on heat transfer and pressure drop were studied. It was concluded that the twisted tape inserts have significant effect on enhancing heat transfer rate. However, the pressure drop also increases. Eiamsa-ard et al. (2010) investigated experimentally heat transfer, flow friction and thermal performance factor characteristics in a tube fitted with delta winglet twisted tape, using water as working fluid. Influences of the oblique delta-winglet twisted tape (O-DWT) and straight delta-winglet twisted tape (S-DWT) arrangements are also described. The experiments are conducted using tapes with three twist ratios ($y/w = 3, 4$ and 5) and three depth of wing cut ratios ($DR = d/w = 0.11, 0.21$ and 0.32) over a Reynolds number range of $3,000-27,000$ in a uniform wall heat flux tube. The obtained results shows that mean Nusselt number and mean friction factor in the tube with the delta-winglet twisted tape increases with decreasing twisted ratio (y/w) and increasing depth of wing cut ratio (DR). It is also observed that the O-DWT provides more effective turbulence giving higher heat transfer coefficient than the S-DWT. Sarada et al. (2010) presented experimental results for the augmentation of turbulent flow heat transfer in a horizontal tube by means of varying width twisted tape inserts with air as the working fluid. Their results show the enhancement of heat transfer with twisted tape inserts as compared to plain tube varied from 36 to 48 % for full width (26 mm) and 33 to 39 % for reduced width (22 mm) inserts. Jaiman and Oakley (2010) studied a rough pipe 16" with three geometries that had different depths of roughness for a cryogenic transfer operation. Subsequently, the flow patten and the friction factor for rough pipes type D (Stel et al., 2012) was studied. The results showed the friction factor was a logarithmic function respect to Reynolds number for a constant depth of roughness. Han et al. (2015), optimized heat exchanger with inner corrugated tube. The design parameters used were dimensionless: corrugation pitch (p/D), corrugation height (H/D), corrugation radius (r/D) and Reynolds number (Re). They noted that an increase in heat transfer was against the pressure drop and optimum proposed. Kareem et al. (2015), performed an

experimental and numerical study of the flow of water at low Reynolds number in a spirally corrugated tubes to determine the thermal performance of a new style of corrugation profile. The experimental and simulated results verified the proposed model. The new pipe showed heat transfer enhancement range of 2.4-3.7 times of smooth tube, while the friction factor increased from 1.7 to 2.4.

This summary of important research performed shows the advantages of simulation, as it is able to analyze and solve more complex problems, where the classical equations cannot be used because they have not been developed for these specific cases, therefore the simulation is a good choice to propose novel configurations efficiently.

4. OBJECTIVES

The main goal of this project is to check the effectiveness of ANSYS® to simulate double pipe heat exchangers. To answer this question, several objectives are addressed:

- Learn the use of the simulator ANSYS®.
- Using ANSYS® to simulate a three dimensional double pipe heat exchanger.
- Modeling and simulating flow through a smooth double pipe comparing the simulated results with available experimental data or empirical equations.
- Modeling and simulating for double pipe heat exchanger with inner fins.
- Results interpretation and validation of the results of both simulations compared critically with classical equations.

5. MATERIAL, METHODS AND COMPUTATIONAL STUDY

5.1. MATERIAL

In this project, CFD software (ANSYS® Fluent) is used to find the numerical solution of the complete domain of interest to the governing equations of the fluid flow and heat transfer for double pipe heat exchangers. For the purpose of simulation is used the academic version 16.2. A laptop with Intel Core i7-5500U and 4GB memory was used.

5.2. CFD PROCEDURE

In this section, the procedure followed during the simulation is describes, the procedure is divided into three main steps:

1. PRE-PROCESSING

Pre-processing is the first step to deal with a simulation problem and includes:

- Definition and creation of the geometry and flow region with the help of CAD software.
- Meshing the geometry by dividing the volume into discrete cells.

2. SOLVER

- Selection of fluid properties and the underlying physics is adopted to solve the computational problems – for example, the equations of motion, enthalpy, radiation, species conservation, etc.

- Boundary conditions are specified at inlet, outlet and on the surfaces of geometry according to the specific requirements of the problem. Selection of proper boundary conditions are of paramount importance to reach final results.
- Initialization of the iterative procedure involving all the discrete values of the flow properties, e.g. velocity, pressure, temperature, and other transport parameters of interest. The equations are solved iteratively as a steady-state.
- Convergence is monitored for successful computational solution. A converged solution is achieved when the residuals of the difference between two iteration solutions reach below the given convergence criteria.

3. POST-PROCESSING

Post-processing stage is characterized by:

- Post-processing shows the computational results through graphical displays and values of the flow properties, providing the results of various flow phenomenon, velocity contours, pressure contours, temperature contours, etc.

5.2.1. PRE-PROCESSING

5.2.1.1. Geometry

The first step in the simulation process is to create the geometry, therefore creating design models is a core part of the product development process. These models can be geometric forms representing actual design or approximations of the designs using simplified components. The ANSYS® DesignModeler module has been the main tool used in this case to create the geometry. The ANSYS® DesignModeler application is a parametric feature-based solid modeler designed for an intuitive and quick drawing of 2D sketches (lines, arcs, circles...), modeling 3D parts (surfaces and bodies), or uploading 3D CAD models for engineering analysis preprocessing. This part of the pre-preprocessing can be performed via external CAD Design applications, transferring the data to ANSYS® later. The DesignModeler application is quite intuitive, as shown in Figure 2.

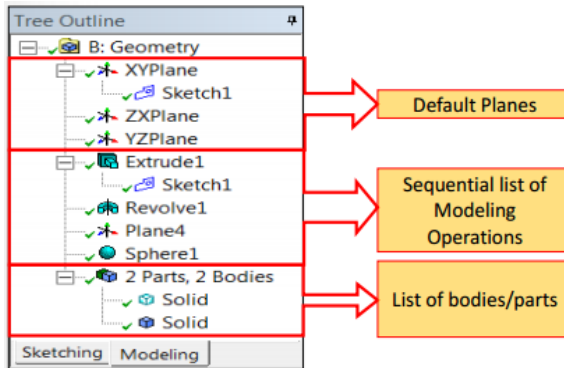


Figure 2. Tree Outline window

By default, ANSYS® DesignModeler application starts in modeling mode, meaning Tree Outline is displayed and the Modeling tab is displayed below at the bottom of the Tree Outline window. Selecting the Sketching tab will display the Sketching toolboxes in the same region of the interface. The default mode changes via the Display category in the miscellaneous section of the Options panel.

A sketch is always required as a first step when a new model is created. All sketches are attached to unique planes. Only a single sketch can be worked on at a time, it is called “active sketch”. Each sketch has a single body, which is defined as “Solid” (in cases of structural analysis) or “Fluid” (flow analysis).

Then, there is a list of the main tools that have been used to generate the geometry (ANSYS®, 2016):

- Revolve: it serves to create a revolved feature. The active sketch is the default but can be changed using the Tree Outline by selecting the desired sketch, a plane from face (boundary used) or Named Selection features or Point Features in the Tree Outline. Geometric entities such as faces, edges, vertices or point feature points are suitable as input for the Revolve feature. A sketch or a plane or combination of Named Selection features, point features and/or geometry entities are selected as input geometry. The Revolve feature uses faces (its edges are actually used), edges, surface bodies (treated like faces), line bodies (treated like edges) as input geometric entities as well as entities from named selections. Point feature points and vertices can also be selected as input geometry. If the input

geometry contains closed sets of edges and/or faces, only the closed sets of edges and/or faces are used for revolution. If there are no closed sets of edges and/or faces, then only open sets of edges are used for revolution. Vertices and point feature points are used when nothing else is selected. If there is a disjoint line in the sketch, it is chosen as the default axis of revolution. The axis of revolution can be a Direction Reference selected from a plane, 2D sketch edge, 3D model edge, face or two points. Further, the Details View are used to change the angle of revolution, the feature direction, and modeling operation: Add, Cut, Slice, Imprint, or Add Frozen. For this project the options Add Material and Add Frozen are used.

- i. Add Material: creates material and merges it with the active bodies in the model. This option is always available.
 - ii. Add Frozen: creates material, but adds it to the model as frozen bodies, without merging them with other bodies in the model. This allows, for example, to import a model as a set of frozen bodies without the need to manually apply the Freeze feature afterwards. This option is always available.
- Symmetry: this tool is used to define a symmetry model. The feature takes either all the bodies or selected bodies of the model as input and accepts up to three symmetry planes. The user can choose either full or partial models to work with. When a full model is used, the selected symmetry planes slice off the model and only a portion of the model is retained. The valid body types for this feature are surface and solid.
 - Generate: to update the model after any number of changes in the model's feature or sketch/plane dimensions, or changes in design parameters.
 - Named Selections: to create named selections that can be transferred to the ANSYS® Mechanical application, or used in the creation of some features. Any combination of 3D entities are selectable, including point feature points (PF points). Selections are performed through an Apply/Cancel property called Geometry in the Details View of ANSYS® DesignModeler.

5.2.1.2. Mesh

The geometry previously created is imported to the Meshing module. In this case, for the meshing activity, ANSYS® DesignMeshing (ANSYS®, 2016) is employed. Mesh generation is one of the most critical aspects of simulation. Too many cells may result in long solver runs, and too few may lead to inaccurate results.

The partial differential equations that govern fluid flow and heat transfer are not usually amenable to analytical solutions, except for very simple cases. Therefore, in order to analyze fluid flow (Löhner, 2002; Donea and Huerta, 2003), flow domains are split into smaller sub domains (made up of geometric primitives like hexahedral and tetrahedral in 3D and quadrilaterals and triangles in 2D): the governing equations are then discretized and solved inside each of these sub domains (Patel et al., 2011; Ruprecht et al., 2014). Typically, one of three methods is used to solve the approximate version of the system of equations: finite volumes (FVM), finite elements (FEM), or finite differences (FDM) (Peyret, 1996). The computational domain is divided into a number of small domains (discretization) to solve the flow problems within the domain geometry. These are also called as grids or cells, as shown in Figure 3, where the fluid flows are solved numerically to get the discrete values of flow properties like velocity, pressure, temperature and other transport phenomenon as per requirement.

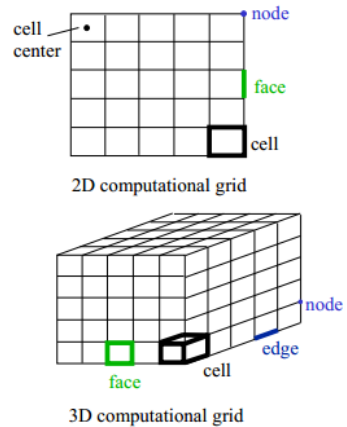
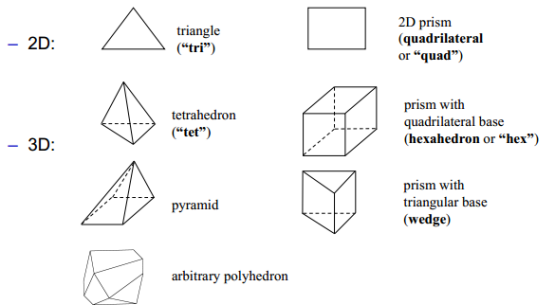


Figure 3. Grid terminology

The stability and accuracy of the computation depends on the quality of the mesh, which plays a vital role. Skewness, aspect ratio and smoothness are the major attributes associated with mesh quality. Ensuring the quality of the grid is essential regardless of the kind of mesh employed in the domain. Different quality criteria are usually evaluated depending on the type of cell in the mesh (tetrahedral, hexahedral, polyhedral, etc, Figure 4). The mesh is acceptable if it has a skewness range of 0.75-0.8 for 3D geometry while mesh with skewness greater than 0.85 is regarded as worst mesh. The measure of the stretch of a cell is referred to as the aspect ratio. It is defined as the ratio of the maximum distance between the cell centroid and face centroids to the minimum distance between the nodes of the cell. Aspect ratio of 1.0 is regarded as the best

aspect ratio and it is an indication that the cell is nicely squared and or equal edge length of any shape. The smoothness of the edge or rather the change in the size of the cell must be gradual and a change of more than 20% from a cell to the next cell is not acceptable. Where the cells vary largely in size, the smoothness will be very bad, making the solution hard to converge. The element quantity and the node are very important since they reflect in the final outcome and the computational time which also reflects computational cost. The higher the meshing element, the better the final outcome but it takes longer computational time to complete the simulation. The



acceptable mesh quality is obtained from the solution with both acceptable final result and as well as the acceptable computational time (Kareem et al., 2015).

Figure 4. Typical cell shapes

In summary, appropriate choice of grid type depends on: geometric complexity, flow field and cell and element types supported by solver. Design and construction of a quality grid is crucial to the success of the CFD analysis. Strike a balance between results and analysis time is the main goal.

The following features has been used in the meshing of the geometry (ANSYS®, 2016):

- **Physics Preference:** to establish how Workbench performs meshing based on the specified physics of the analysis type. Available options are: Mechanical, Electromagnetic, CFD, and Explicit. The value of the Physics Preference option sets the default for various meshing controls.
- **Solver Preference:** can be CFX, Fluent, or Polyflow. Based on the value, the Meshing application sets certain defaults that result in a mesh that is more favorable to the CFX, Fluent, or Polyflow solver, respectively.
- **Relevance:** to control the *fineness* of the mesh for the entire model. To indicate a preference toward high speed (-100) or high accuracy (+100) solutions, the slider located in the Details View is used, clicking the Relevance value. This number is

used in the report to document the relevance setting. The finer the mesh, the more accurate the result. A coarse mesh is less accurate. However, a finer mesh uses more elements, more time, and ultimately, more system resources.

- **Relevance Center:** sets the gauge of the Relevance: slider control in the Default group. Options are Coarse, Medium, and Fine. The default value is set automatically according to the Physics Preference setting as described above under the Default Group.
- **Smoothing:** to improve element quality by moving locations of nodes with respect to surrounding nodes and elements. The Low, Medium, or High option controls the number of smoothing iterations along with the threshold metric where the mesher starts smoothing.
- **Element Size:** to specify the element size used for the entire model. This size is used for all edges, faces, and body meshing. This option does not appear when Use Advanced Size Function is on.
- **Aspect Ratio:** to set stretches the rectangle in a direction parallel to the grid axes. If a value less than one is entered, the grid is stretched in one direction. If a value greater than one is entered, the grid is stretched in the direction perpendicular to the previous direction.
- **Inflation:** useful for CFD boundary layer resolution, electromagnetic air gap resolution or resolving high stress concentrations for structures.

5.2.2. SOLVER

Once the geometry and the mesh has been properly stated, the physical model must be defined. The tool used is ANSYS® Fluent 16.2, which provides comprehensive modeling capabilities for a wide range of incompressible and compressible, laminar and turbulent fluid flows problems. In ANSYS® Fluent Software, a broad range of mathematical models for transport phenomena (like heat transfer) is combined with the ability to model complex geometries. Also, various modes of heat transfer can be modeled, including natural, forced, and mixed convection with or without conjugate heat transfer, porous media, and so on. This software is especially useful for modeling multiple stages in turbomachinery applications, for example, is also provided, along with the mixing plane model for computing time-averaged flow fields (ANSYS®, 2016). The

parameters that determine the simulations results and, therefore, considered more relevant at this point, are listed below:

5.2.2.1. Solver algorithms

There are two kinds of solvers available in Fluent: pressure-based solver or density-based solver. Historically, the pressure-based approach was developed for low-speed incompressible flows, while the density-based approach was mainly used for high-speed compressible flows. However, both methods have been extended and reformulated to solve and operate for a wide range of flow conditions. In both methods the velocity field is obtained from the momentum equations. In the density-based approach, the continuity equation is used to obtain the density field while the pressure field is determined from the state equation. On the other hand, in the pressure-based approach, the pressure field is extracted by solving a pressure or pressure correction equation which is obtained by manipulating continuity and momentum equations. The two numerical methods employ a similar discretization process (finite-volume), but the approach used to linearize and solve the discretized equations is different (ANSYS®, 2016).

Otherwise, the coupled set of governing equations in ANSYS® Fluent is discretized in time for both steady and transient calculations. In the steady case, it is assumed that time marching proceeds until a steady-rate solution is reached. Either an implicit or an explicit time-marching algorithm accomplishes temporal discretization of the coupled equations.

5.2.2.2. Models

ANSYS® Fluent uses different models to describe the effects of turbulent fluctuations: standard, RNG and realizable k - ϵ models. All three models have similar forms, with transport equations for k and ϵ . The major differences in the models are as follows: the method of calculating turbulent viscosity, the turbulent Prandtl numbers governing the turbulent diffusion of k and ϵ and the generation and destruction terms in the ϵ equation. Besides, Fluent provides two turbulence options within the context of the Reynolds stress models (RSM) (ANSYS®, 2016).

5.2.2.3. Boundary conditions

Boundary conditions are a set of properties or conditions on surfaces of domains, and are required to fully define the flow simulation. They are, therefore, a critical component of Fluent simulations and it is important that they are specified appropriately. The positive side of things is that the user does not have to deal directly with the fluid flow equations (Navier Stokes equations),

because ANSYS® provides an interface tools to simplify the process of assigning boundary conditions.

The boundary types available in Fluent are classified as follows (ANSYS®, 2016):

- Flow inlet and exit boundaries: pressure inlet, velocity inlet, mass flow inlet, and inlet vent, intake fan, pressure outlet, pressure far-field, outflow, outlet vent, and exhaust fan.
- Wall, repeating, and pole boundaries: wall, symmetry, periodic, and axis.
- Internal face boundaries: fan, radiator, porous jump, wall, and interior.
- Cell zones consist of fluids and solids, with porous media and 3D fans treated as a type of fluid zone.

5.2.2.4. Solution method

Choose the solution method corresponds to the last stage of the solver. ANSYS® Fluent works with a solver setting called “Pressure-Velocity Coupling”. This solver setting refers to the numerical algorithm which uses a combination of continuity and momentum equations to derive an equation for pressure (or pressure correction) when using the pressure-based solver.

Five algorithms are available in Fluent:

- Semi-Implicit Method for Pressure-Linked Equations (SIMPLE): the default scheme, robust.
- SIMPLE-Consistent (SIMPLEC): allows faster convergence for simple problems (e.g., laminar flows with no physical models employed).
- Pressure-Implicit with Splitting of Operators (PISO): useful for unsteady flow problems or for meshes containing cells with higher than average skewness.
- Fractional Step Method (FSM) for unsteady flows: used with the NITA scheme; similar characteristics as PISO.
- Coupled (or pressure-based coupled solver).

In addition, ANSYS® Fluent package allows to set other aspects such as: interpolation methods and the type of discretization.

5.3. COMPUTATIONAL STUDY

5.3.1. GOVERNING EQUATIONS

The fundamental principles governing the flow and heat transfer in the double pipe heat exchanger are expressed in terms of the following partial differential equations. The mass, momentum and the energy equations are solved for steady state solutions on the entire domain with the application of finite volume method. The methodology used here is similar to that adopted by Lochan et al. (2014) in the numerical analysis of double pipe heat exchanger using heat transfer augmentation techniques.

The governing equation of the flow problem in the vectors forms as follows:

Continuity equation

$$\nabla \cdot \rho \vec{V} = 0 \quad (1)$$

Momentum equation

$$\nabla \cdot (\rho \vec{V} \vec{V}) = -\nabla P + \nabla \cdot (\mu \nabla^2 \vec{V}) \quad (2)$$

Energy equation

$$\nabla \cdot (\rho \vec{V} C_p T) = \nabla \cdot (k \nabla T) \quad (3)$$

The standard k- ϵ model is adopted here to close the governing equations:

$$\begin{aligned} \frac{\partial}{\partial t} (\rho k) + \frac{\partial}{\partial x_i} (\rho k u_i) &= \frac{\partial}{\partial x_j} \left[\left(\mu + \frac{\mu_t}{\sigma_k} \right) \frac{\partial k}{\partial x_j} \right] + G_k + G_b - \rho \epsilon - Y_M + S_k \quad (4) \\ \frac{\partial}{\partial t} (\rho \epsilon) + \frac{\partial}{\partial x_i} (\rho \epsilon u_i) &= \frac{\partial}{\partial x_j} \left[\left(\mu + \frac{\mu_t}{\sigma_\epsilon} \right) \frac{\partial \epsilon}{\partial x_j} \right] + C_{1\epsilon} \frac{\epsilon}{k} (G_k + C_{3\epsilon} G_b) - C_{2\epsilon} \rho \frac{\epsilon^2}{k} + S_\epsilon \quad (5) \end{aligned}$$

where μ_t is the turbulent or eddy viscosity, G_k represents the generation of turbulence kinetic energy due to the mean velocity gradients, G_b is the generation of turbulence kinetic energy due to buoyancy and Y_M represents the contribution of the fluctuating dilation in compressible turbulence to the overall dissipation rate. $C_{1\epsilon}$, $C_{2\epsilon}$, and $C_{3\epsilon}$ are constants. σ_k and σ_ϵ are the turbulent Prandtl numbers for k and ϵ , respectively. S_k and S_ϵ are user-defined source terms.

In the present model, it is assumed that:

- i. The flow is steady and 3D developing flow.
- ii. The working fluid in a single phase, and its properties remain constants.
- iii. Gravitational forced is neglected.

The CFD code Fluent is based on the finite volume method on a collocated grid and general purpose software to analyze problems in fluid dynamics. Fluent was used to solve equations for the fluid flow and heat transfer analyses in this case.

5.3.2. THE ANALYSIS DOMAIN

One smooth and one finned tube were modelled to be simulated numerically. Both geometry considered in the computation are 3D.

5.3.2.1. Details double pipe heat exchanger

A schematic view of the configuration of the double tube heat exchanger is shown in Figure 5. The dimensions chosen have been provided by Serth (2007) in the appendix B.2 related to the “Design of double pipe exchanger”. The geometric parameter for the numerical analysis is shown in Table 1. The smooth double pipe is modelled according to the methods described by Serth (2007) for the purpose of model validation.

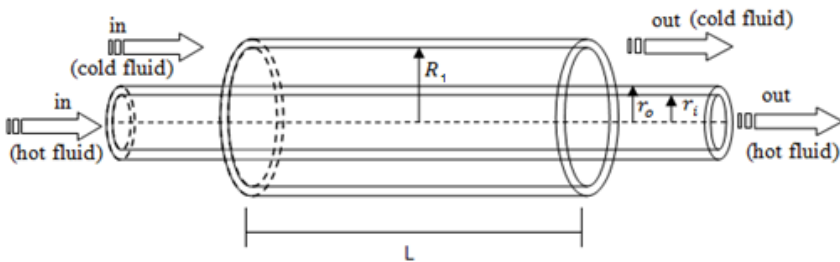


Figure 5. Experimental model double tube heat exchanger

Table 1. Parameter used for the double pipe study

	Parameter	Value
INNER PIPE	Inside radius (r_i)	2.85 cm
	Outside radius (r_o)	3.02 cm
OUTER PIPE	Inside radius (R_1)	4.23 cm
	Outside radius (R_2)	4.45 cm
	Pipe length (L)	1000 and 100 cm

5.3.2.2. Details double pipe heat exchanger with fins

The finned double pipe heat exchanger has the same dimensions as the smooth double pipe, but adding longitudinal fins on the outer surface of the inner tube, as shown in Figure 6. The flow is more complicated in this section than the previous one, so the computational accuracy is mainly affected by the mesh density. Based on this principle, in order to save the computational time, meanwhile ensuring good precision, the length is reduced from 10 meters to 1 meter. The final parameters are shown in Table 2.

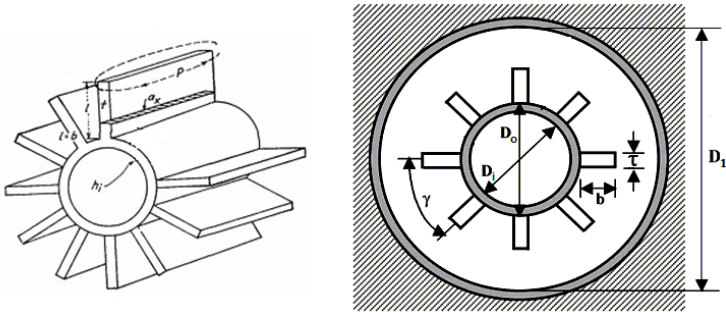


Figure 6. Experimental model double tube heat exchanger with fins

Table 2. Parameter used for the double pipe with fins study

	Parameter	Value
INNER PIPE	Inside diameter (D_i)	5.70 cm
	Outside diameter (D_o)	6.03 cm
OUTER PIPE	Inside diameter (D_1)	8.47 cm
	Outside diameter (D_2)	8.89 cm
	Angle between fins (γ)	9 °
	Number of finned pipes (n_f)	1
	Number of fins on each pipe (N_f)	40
	Fin height (b)	0.61 cm
	Fin thickness (τ)	0.10 cm
	Weighted efficiency (η_w)	0.48
	Fin efficiency (η_f)	0.33

Table 2. Parameter used for the double pipe with fins study (*continued*)

Parameter	Value
Prime surface (A_{prime})	0.15 m ²
Surface area of all fins (A_{fins})	0.53 m ²
Total heat transfer surface (A_{TOT})	0.68 m ²
Pipe length (L)	100 cm

5.3.3. NUMERICAL MODELING

5.3.3.1. Heat transfer coefficient calculation of simulation

All of the heat is assumed to be transferred between the streams at their average temperatures, t_{ave} for the fluid in the inner pipe and T_{ave} for the fluid in annulus, Eq. (6) is satisfied for heat transfer process of heat exchangers:

$$Q = h_i \cdot A_i \cdot (t_{ave} - T_w) = h_o \cdot A_o \cdot (T_w - T_{ave}) \quad (6)$$

Energy balance for finned pipes is defined by

$$\begin{aligned} Q &= h_i \cdot A_i \cdot (t_{ave} - T_p) = h_o \cdot \eta_w \cdot A_{TOT} \cdot (T_p - T_{ave}) = \\ &= h_o \cdot A_{TOT} \cdot (T_{wtd} - T_{ave}) \end{aligned} \quad (7)$$

The heat transfer is calculated from

$$Q = \dot{m}_h \cdot C_p \cdot (T_1 - T_2) = \dot{m}_c \cdot C_p \cdot (t_2 - t_1) = U_D \cdot A \cdot \Delta T_{ml} \quad (8)$$

Combining Eqs. (6), (7) and (8), the heat transfer coefficients can be determined in each case. T_{ave} , t_{ave} , T_w , T_{wtd} and T_p can be obtained from simulation results. A_i , A_o , A_{TOT} are decided by the model, where A_{TOT} is:

$$A_{TOT} = A_{fins} + A_{prime} \quad (9)$$

5.3.3.2. Double pipe correlations used for validation

In heat transfer validation for reliability of numerical simulation, two kinds of practical engineering correlations of the heat transfer coefficient are used, Eq. (10) from Serth (2007) and Eqs. (11) and (12) from Levenspiel (1993).

For turbulent flow ($Re \geq 10^4$), the following equations are used:

$$Nu = \frac{h_i \cdot D_i}{k} = 0,023 \cdot Re^{0.8} \cdot Pr^{\frac{1}{3}} \cdot \left(\frac{\mu}{\mu_w}\right)^{0.14} \quad (10)$$

Eq. (10) is used for both pipes and annuli, with the equivalent diameter replacing D_i , in the case of an annulus.

$$Nu = \frac{h_i \cdot D_i}{k} = 0,023 \cdot \left[1 + \left(\frac{D_i}{L}\right)^{0.7}\right] \cdot Re^{0.8} \cdot Pr^{\frac{1}{3}} \cdot \left(\frac{\mu}{\mu_w}\right)^{0.14} \quad (11)$$

For heat flow to the wall of the inner tube:

$$Nu = \frac{h_o \cdot D_e}{k} = 0,02 \cdot Re^{0.8} \cdot Pr^{\frac{1}{3}} \cdot \left(\frac{D_1}{D_0}\right)^{0.53} \cdot \left(\frac{\mu}{\mu_w}\right)^{0.14} \quad (12)$$

where Re is the Reynolds number of fluid, which is defined by Eq. (13):

$$Re = \frac{4 \cdot \dot{m}}{\pi \cdot D_e \cdot \mu} \quad (13)$$

For hydraulic calculations, the correlation of Serth (2007) has been used. According to this, the pressure drop is expressed in terms of the friction factor, f , as:

$$\Delta P_f = \frac{f \cdot L \cdot G^2}{7.50 \times 10^{12} \cdot D_i \cdot s \cdot \left(\frac{\mu}{\mu_w}\right)^{0.14}} \quad (14)$$

where s is the specific gravity of liquids, which is usually referenced to water at 4°C, which has a density 62.43 lbm/ft³. L and D_i are expressed in ft and G in lbm/h·ft², the units of ΔP_f are psi. Eq. (14) is also applicable to flow in the annulus of a double pipe exchanger if the pipe diameter, D_i , is replaced by the equivalent diameter, D_e .

The friction factor to be used with Eq. (14) can be computed as follows. For turbulent flow with $Re \geq 3000$, the following equation is used for both the pipe and the annulus:

$$f = 0.3673 \cdot Re^{-0.2314} \quad (15)$$

To calculate the pipe wall temperature:

$$T_w = \frac{h_i \cdot t_{ave} + h_o \cdot \left(\frac{D_o}{D_i}\right) \cdot T_{ave}}{h_i + h_o \cdot \left(\frac{D_o}{D_i}\right)} \quad (16)$$

The overall heat transfer coefficient calculated from the following equation

$$U_D = \left[\frac{D_o}{h_i \cdot D_i} + \frac{D_o \cdot \ln\left(\frac{D_o}{D_i}\right)}{2 \cdot k_{pipe}} + \frac{1}{h_o} \right]^{-1} \quad (17)$$

5.3.3.3. Correlations for double pipe with fins used for validation

In this case, for turbulent flow ($Re \geq 10^4$) for inner pipe, the Eqs. (10) and (11) are used too. Also, the following equation (Sinnott and Towler, 2012) has been adapted from the data given by Tagle and Ferguson (Serth, 2007) and it is developed specifically for water:

$$h_i = \frac{4200 \cdot (1.35 + 0.02 \cdot T) \cdot u^{0.8}}{D_i^{0.2}} \quad (18)$$

where T is expressed in °C, u in m/s and D_i in mm.

However, for the finned annulus with transition region ($2,100 < Re < 10^4$) the Eq. (19) from Levenspiel (1993) and Eq. (20) from Serth (2007) are used to calculate the heat transfer coefficients:

$$Nu = \frac{h_o \cdot D_e}{k} = 0.11 \cdot \left[Re^{2/3} - 125 \right] \cdot Pr^{1/3} \cdot \left[1 + \left(\frac{D_e}{L} \right)^{2/3} \right] \cdot \left(\frac{\mu}{\mu_w} \right)^{0.14} \quad (19)$$

$$h_o = j_H \cdot \left(\frac{k}{D_e} \right) \cdot Pr^{1/3} \quad (20)$$

Where the flow area and equivalent diameter for a finned annulus are

$$A_f = \frac{\pi}{4} \cdot (D_1^2 - n_t D_0^2) - n_t \cdot N_f \cdot b \cdot \tau \quad (21)$$

$$D_e = \frac{4 \cdot A_f}{\pi \cdot (D_1 + n_t D_0) + 2 \cdot n_t \cdot N_f \cdot b} \quad (22)$$

At low Reynolds numbers, j_H depends on the fin number according to correction factor. For Reynolds numbers above 1,000, the effect of fin number diminishes and j_H without the correction factor can be used. In this project, the Reynolds number for the finned annulus is around 6,000. According to this value of Reynolds, $j_H \approx 17$ (using Figure 4.4 in the Chapter 4 related to the "Design of double pipe exchanger" by Serth (2007)).

To determine the pressure drop and the friction factor for both pipe and finned annulus, Eq. (14) and (15) are used.

Wall temperature for finned pipe is calculated using a weighted average temperature, T_{wtd} , of the extended and prime surfaces, Eq. (23). Eq. (24) is used to calculate the wall temperature for the fluid in the inner pipe, T_p .

$$T_{wtd} = \frac{h_i \cdot \eta_w \cdot t_{ave} + \left[h_i \cdot (1 - \eta_w) + h_o \cdot \eta_w \cdot \left(\frac{A_{TOT}}{A_i} \right) \right] \cdot T_{ave}}{h_i + h_o \cdot \eta_w \cdot \left(\frac{A_{TOT}}{A_i} \right)} \quad (23)$$

$$T_p = \frac{h_i \cdot t_{ave} + h_o \cdot \eta_w \cdot \left(\frac{A_{TOT}}{A_i} \right) \cdot T_{ave}}{h_i + h_o \cdot \eta_w \cdot \left(\frac{A_{TOT}}{A_i} \right)} \quad (24)$$

Where η_w is the weighted efficiency (Eq. 25) of the entire finned surface, which depends on the fin efficiency (Eq. 26), η_f , and its form.

$$\eta_w = \frac{\eta_f \cdot A_{fins} + A_{prime}}{A_{TOT}} \quad (25)$$

$$\eta_f = \frac{\tanh(m \cdot b_c)}{m \cdot b_c} \quad (26)$$

where

b_c : corrected fin height

m : parameter that depends on fin thermal conductivity and heat-transfer coefficient in annulus.

The overall heat transfer coefficient is calculate using the following expression:

$$U_D = \left[\frac{A_{TOT}}{h_i \cdot A_i} + \frac{A_{TOT} \cdot \ln\left(\frac{D_o}{D_i}\right)}{2 \cdot \pi \cdot k_{pipe} \cdot L} + \frac{1}{h_o \cdot \eta_w} \right]^{-1} \quad (27)$$

Viscosity wall determinate from Sinnott and Towler (2012) in all cases, as follows

$$\text{Log}[\mu_w] = [VISA] \cdot \left[\left(\frac{1}{T} \right) - \left(\frac{1}{VISB} \right) \right] \quad (28)$$

where VISA and VISB are constant: 658.25 and 283.16 for the water fluid, respectively. These values are obtained from Reid et al. (1977). T is expressed in K and μ_w in mNs/m².

5.3.4. NUMERICAL METHODOLOGY

The software DesignModeler is a geometric modeling and grid generation tool used with Fluent. In order to define the geometry of the system, the model drawing is created and meshed by using ANSYS®.

5.3.4.1. Design Modeler

Both the double pipe heat exchanger and one finned are drawn by the creation of four different solids bodies, one for each diameter (from the center coordinate to corresponding dimension): internal diameter of inner pipe (D_i), external diameter of inner pipe (D_o), internal diameter of outer pipe (D_1) and external diameter of outer pipe (D_2). In the case of the double pipe with fins is added a new solid body on the external surface of the inner pipe by creating a new sketch used to draw the fins. On the other hand, in this project, the cylinder is simplified through the use of symmetric planes to save computational cost in the stage of meshing and Cartesian coordinates are employed.

A list of the features used for the creation of each part:

- Details of Symmetry 1: Target Bodes: All Bodies. Symmetry Plane: YZPlane.

DETAILS DOUBLE PIPE

Surface between coordinate origin and D_i :

- Details of Body1: inner_fluid.
- Revolve1: Sketch 1. Operation: Add Material.

Surface between coordinate origin and D_0 :

- Details of Body2: inner_pipe.
- Revolve2: Sketch 2. Operation: Add Frozen.

Surface between coordinate origin and D_1 :

- Details of Body3: outer_fluid.
- Revolve3: Sketch 3. Operation: Add Frozen.

Surface between coordinate origin and D_2 :

- Details of Body3: outer_pipe.
- Revolve4: Sketch 4. Operation: Add Frozen.

DETAILS DOUBLE PIPE WITH FINS

Surface between coordinate origin and D_i :

- Details of Body1: inner_fluid.
- Extrude1: Sketch 1. Operation: Add Material.

Surface between D_i and D_0 + additional surface on D_0 , corresponding to the fins:

- Details of Body2: inner_pipe + fins.
- Extrude2: Sketch 2. Operation: Add Frozen.

Surface between D_0 and D_1 :

- Details of Body3: outer_fluid.

- Extrude3: Sketch 3. Operation: Add Frozen.

Surface between D₁ and D₂:

- Details of Body3: outer_pipe.
- Extrude4: Sketch 4. Operation: Add Frozen.

5.3.4.2. Mesh

The mesh configuration of three different geometries appear in this section:

- i. Double tube of 10 meter lengths used to validate the model.
- ii. Double tube of 1 meter length (improved mesh).
- iii. Double tube with fins of 1 meter length.

Finned double tube (iii) is a more complex geometry, which requires more computational cost, therefore it is necessary to reduce the length and make a more accurate meshing. The double tube (i) is reduced from 10 to 1 (ii) meter to compare it with the finned one. The accuracy of mesh used is similar to compare the results under similar conditions.

The parameters used in each case are detailed below:

DETAILS DOUBLE PIPE

Display:

- Physics Preference: CFD.
- Solver Preference: Fluent.
- Relevance: 100.

Sizing:

- Use Advanced Size Function: ON: Curvature.
- Relevance Center: Fine.
- Smoothing: High.

Inflation:

- Use Automatic Inflation: Program Controlled.
- Inflation Option: Smooth Transition.
- Transition Ratio: 0.272.

- Maximum Layers: 5.
- Growth Rate: 1.2.

Furthermore, inflation is created on regions near the wall as shown in Figure 7, because the heat exchanger takes place mainly on these areas.

Mesh control:

- Inflation (A) and (B):
- Inflation Option: Smooth Transition.
- Maximum Layers: 4.
- Growth Rate: 1.2.

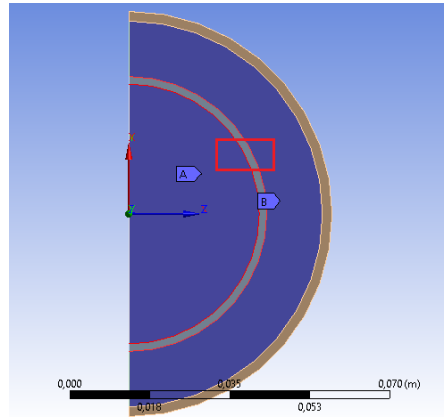


Figure 7. Surface on which inflation applies

DETAILS DOUBLE PIPE (improved mesh)

Display, sizing, inflation automatic and manual inflation configuration are maintained, but the following is incorporated:

Edge Sizing (A), (C), (D), (F):

- Type: Number of divisions: 95.
- Behavior: Hard.

Edge Sizing (B):

- Type: Number of divisions: 95.
- Behavior: Hard.
- Bias Type: Bias Factor: 5.

Edge Sizing (E):

- Type: Number of divisions: 30.
- Behavior: Hard.
- Bias Type: Bias Factor: 5.

Sweep Method:

- Geometry: Outer fluid.
- Free Face Mesh Type: Quad/Tri.

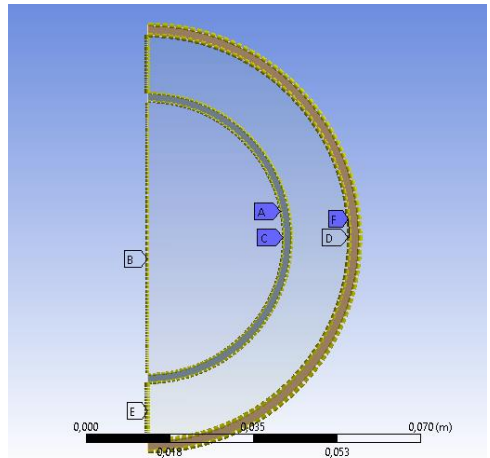


Figure 8. Surface that shows the BIAS distributions

The Edge Sizing with number of divisions and hard behavior are used to force the program to perform a regular mesh. Each body is meshed individually. All contact surfaces have the same number of divisions (Figure 8), hence there is a regularity in the mesh. Furthermore, a BIAS factor (or growth factor) is applied: the mesh elements near the wall is five times smaller than the elements of the center, leading to a more refined mesh. The sweep applied on the outer fluid helps keep the regularity in the nodes along the geometry.

To maintain regularity mesh in the longitudinal profile, as shown in Figure 9:

Edge Sizing (A), (B), (C), (D):

- Type: Number of divisions: 80.
- Behavior: Hard.

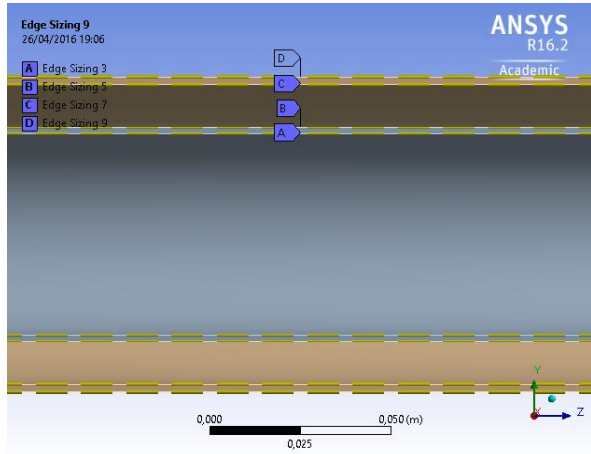


Figure 9. A sector of symmetry plane where Edge Sizing is applied

DETAILS DOUBLE PIPE WITH FINS

Display:

- Physics Preference: CFD.
- Solver Preference: Fluent.
- Relevance: 100.

Sizing:

- Use Advanced Size Function: ON: Curvature.
- Relevance Center: Coarse.
- Smoothing: Medium.

Inflation:

- Use Automatic Inflation: Program Controlled.
- Inflation Option: Smooth Transition.
- Transition Ratio: 0.272.
- Maximum Layers: 5.
- Growth Rate: 1.2.

The fins hinder the meshing, hence the automatic meshing is not useful. Therefore, the overall geometry is sectioned into simpler geometries and mesh them individually, as shown in Figure 10. The features used are:

Edge Sizing (A):

- Type: Number of divisions: 2.
- Behavior: Hard.

Edge Sizing (B), (F):

- Type: Number of divisions: 3.
- Behavior: Hard.

Edge Sizing (C), (H), (I):

- Type: Number of divisions: 95.
- Behavior: Hard.

Edge Sizing (J):

- Type: Number of divisions: 95.
- Behavior: Hard.
- Bias Type: Bias Factor: 5.

Edge Sizing (D), (E), (G):

- Type: Number of divisions: 4.
- Behavior: Hard.

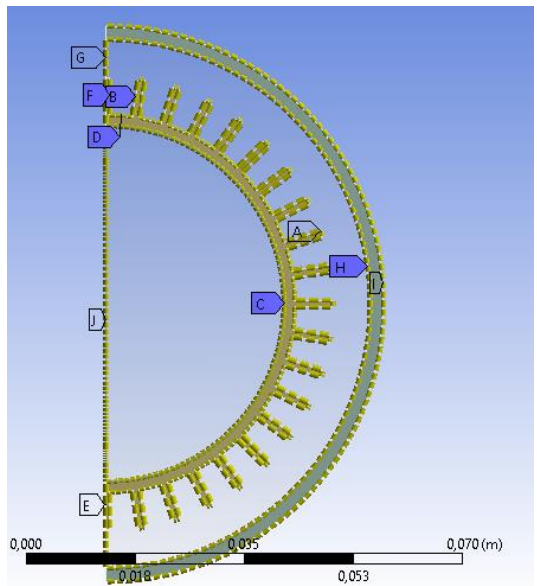


Figure 10. Surface with fins that shows the custom meshing

Multizone:

- Geometry: Inner pipe.
- Mapped Mesh Type: Hexa.

Multizone:

- Geometry: Outer fluid.
- Mapped Mesh Type: Hexa/Prism.

Inner pipe and outer fluid are meshed separately using “Multizone” to ensure conformal mesh. The “Multizone” strategy for meshing provides multi-level sweep with automatic decomposition of geometry into mapped (structured) and free (unstructured) regions. This is seen in more detail at the results chapter.

As in the previous case, the longitudinal profile is meshing as follows:

Edge Sizing (A), (B), (C), (D):

- Type: Number of divisions: 80.
- Behavior: Hard.

5.3.4.3. Solver

TURBULENCE MODELING

- Type: Pressure-Based.
- Time: Steady.
- Gravity: Off.
- Viscous: k-epsilon, Standard, Enhanced Wall Treatment.
- Energy: On.

The pressure based solver is applied to a wide range of flow regimes from low speed incompressible flow to high-speed compressible flow. Also, it requires less memory and allows flexibility in the solution procedure. The numerical simulations are performed with three dimensional, steady-state and turbulent flow system. Standard k-ε model (it takes into account the phenomenon of turbulence and converges quickly to the solution) and “enhanced wall treatment” option are employed and energy equation is included.

MATERIAL MODEL

In all simulations, the working fluid is water in liquid phase with constant density, i.e. incompressible flow. The properties of steam remain constant. The flow rate and Reynolds number based on the averaged velocity are the input for the models. The pipes are made of steel. Fluent has a database that allows selecting a large number of fluids and solids. The water thermos-physical and steel properties are inserted to the Fluent database via editing the fluid and solid property menu, these are summarized in Table 3.

Table 3. Properties of fluid and solid

Variable	Fluid	Solid
ρ [kg/m ³]	998.20	8,030
C_p [J/kg·K]	4,182	502.48
k [W/m·K]	0.60	16.27
μ [kg/m·s]	0.001003	

BOUNDARY CONDITIONS

Fluent recognizes the boundary conditions from the named selections exported from the geometry and meshing. For each case studied there are 5 boundary conditions and a plane of symmetry: 2 inputs, 2 outputs and 1 insulated solid wall. The two stream are flowing in a parallel mode. The flow boundary conditions on both cases are given as follows:

- The inlet conditions for inner fluid (hot water): Velocity inlet, $u_1 = \text{variable}$, $T_1 = 363.15$ K, turbulent specification of the inlet are adopted as turbulence intensity $I = 5\%$ and hydraulic diameter: $D_h = D_i = 0.057$ m;
- The inlet conditions for outer fluid (cold water): Velocity inlet, $u_1 = 0.5$ m/s, $t_1 = 288.15$ K, $I = 5\%$ and hydraulic diameter:
 - $D_h = 0.024$ m (smooth pipe).
 - $D_h = 0.011$ m (pipe with fins).
- The outlet conditions for inner fluid (hot water): $P_2 = 0$ Pa, turbulence specification of the outlet are adopted as turbulence intensity $I = 5\%$ and $D_h = 0.057$ m;

- The outlet conditions for outer fluid (cold water): $p_2 = 0$ Pa, turbulence specification of the outlet are adopted as turbulence intensity $I = 5\%$ and hydraulic diameter:
 - $D_h = 0.024$ m (smooth pipe).
 - $D_h = 0.011$ m (pipe with fins).
- Wall conditions: Adiabatic boundary condition is adopted in the outer wall of annular tube.

SOLVER SETTINGS

SIMPLE algorithm is used for pressure–velocity coupling, and second order upwind scheme is chosen to discretize momentum equation and first order upwind to discretize energy equations.

- Monitors:
 - Residual → Equations Residual → Continuity → Absolute Criteria: 10^{-4} .

One of the most fundamental measures of an iterative solution's convergence is the residual, as it directly quantifies the error in the solution of the equation system. The residual measures the local imbalance of the conserved variable in each control volume in a CFD analysis. For this reason, every cell in the model will have individual residual value for the equations being solved. The residual will never be exactly equal to zero in an iterative numerical solution. However, the lower residual value, the higher the accuracy of the numerical solution. For CFD, while residual levels of 10^{-4} are considered as loosely converged, residual levels of 10^{-5} are considered to be well converged and residual levels of 10^{-6} are considered to be tightly converged, according to Kareem et al. (2015).

- Solution Initialization:
 - Initialization Methods: Hybrid.

Calculating the flow field based on the boundary conditions of the input and output.

- Run Calculation:
 - Number of Iterations: 650.

In the current project, with this number of iterations then that the final residuals of continuity equation, energy equation, x-velocity, y-velocity and z-velocity assures the accuracy of the numerical solution.

6. RESULT AND DISCUSSION

The purpose of this CFD study is to investigate the fluid behaviour in double pipe heat exchanger and check the reliability of ANSYS® software to simulate the heat transfer in these units. The results are structured in two blocks:

1. Simulating flow through a smooth double pipe comparing the simulated results with available experimental and empirical equations.
2. Simulating double pipe heat exchanger with inner fins to investigate the effect of this other configuration respect to the smooth pipe.

In all simulations the hot fluid flows through inner tube and the cold fluid flows through outer tube. The final residual of continuity equation, energy equation, x-velocity, y-velocity and z-velocity are $5.2 \cdot 10^{-4}$, $6.7 \cdot 10^{-8}$, $5.5 \cdot 10^{-8}$, $5.6 \cdot 10^{-8}$ and $5.3 \cdot 10^{-8}$, respectively.

6.1. DOUBLE PIPE HEAT EXCHANGER

6.1.1. Geometry

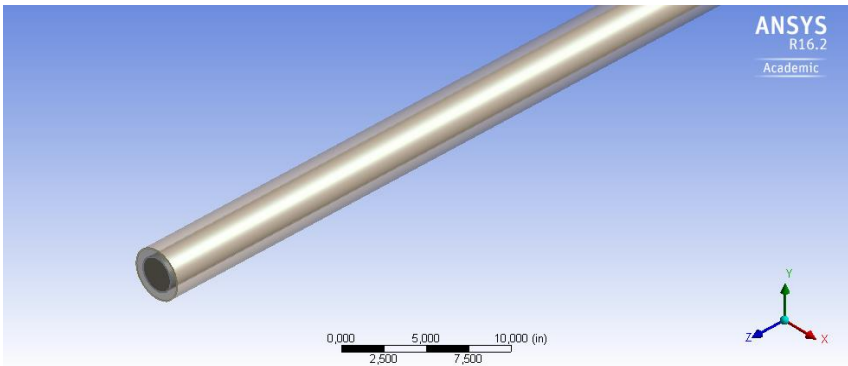


Figure 11. Double pipe geometry

Figure 11 shows a slice of the double pipe 10 meters long created from four Revolve operations (one for each body: inner fluid, thickness of the inner tube, outer fluid and thickness of the outer tube) with a sweep of 360° . Inner fluid is made with the option “Add Material” (yellow area in Figure 12), the other bodies with the option “Add Frozen”.

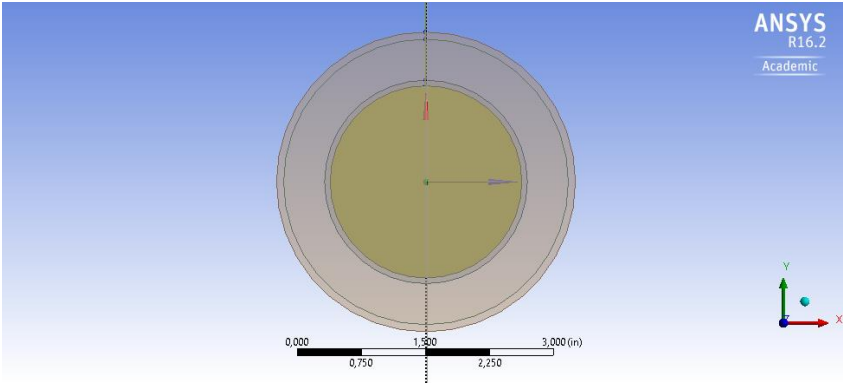


Figure 12. Front view of the double pipe

All bodies are generated from the same origin, so the “Add Frozen” option treats them as independent surfaces being possible to define each boundary condition individually.

6.1.2. Mesh

Figure 13 shows the mesh in the double pipe. A fairly regular grid is observed, with denser areas in regions where a more refined mesh is needed, as for example, near the walls.

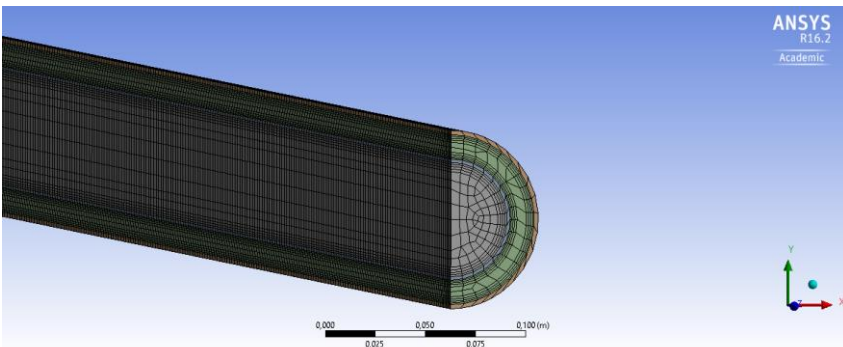


Figure 13. Double pipe mesh

On the other hand, the inflation works as shown in Figure 14, it generates a precise meshing in the regions of fluid-solid interface. ANSYS® qualifies these areas as problematic due to the high perturbations of the flow generated by friction on the walls, where the velocity of the liquid slow down to zero and high temperature gradients are present.

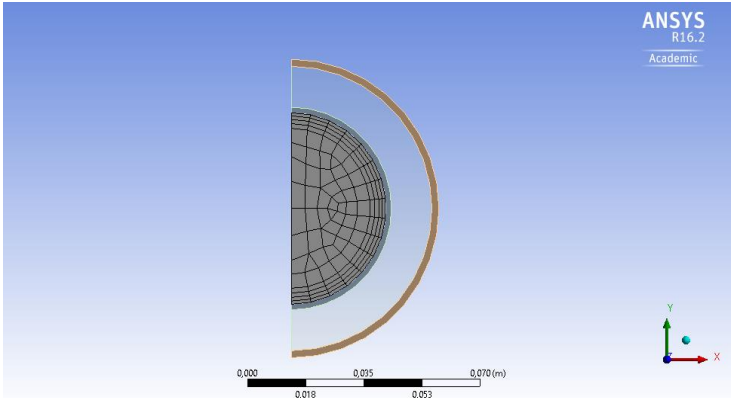


Figure 14. Distribution mesh close to the wall

The whole domain is divided into 365,958 nodes and 332,196 elements. Most elements are hexahedral, as shown in Figure 15, which for 3D meshing usually correspond to structured meshes, characterized by better optimization of the space due to its regularity, furthermore not so many nodes are required and a good convergence towards results is achieved.

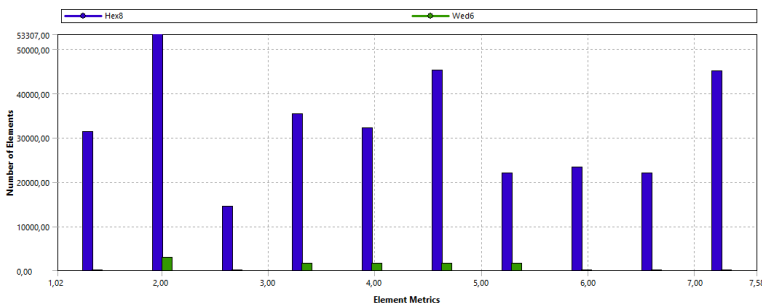


Figure 15. Mesh statistics for the double pipe model

6.1.3. Simulation results of the influence of heat exchanger length

The compared results of heat transfer and pressure drop between numerical simulations and classical engineering correlations at different tube lengths are listed in Table 4. The geometry parameters on inner and outer pipe used in engineering correlations correspond to the description

in Section 5.3.3. The working fluids and its physical properties implemented are the same in the numerical simulations and classical equations. In the Table 4, h_i , h_o and ΔP are the heat transfer coefficients and pressure drop calculated from numerical simulation respectively; h_{iS} , h_{oS} and ΔP_S are the heat transfer coefficients and pressure drop calculated from the correlation of Serth (2007); h_{iL} and h_{oL} are the heat transfer coefficients calculated from the correlation of Levenspiel (1993). U is the overall heat transfer coefficient, which are calculated from combining Eqs. (6) and (8). U_D is the overall theoretical heat transfer coefficient calculated from Eq. (17). The subscript “it” and “ot” indicate inner and outer tube, respectively.

For both inner pipe and outer pipe the working fluid is water and its velocity input is 0.5 m/s. The hot fluid flows through the inner tube and its Prandtl number is 1.98 and Reynolds number is 86,600. The cold fluid flows through the outer tube and its Pr is 6.01 and Re is 14,000. The analysis is done for parallel flow configuration. The result of simulation is provided to carry out the detailed analysis of fluid flow and heat transfer, which is shown as follows.

Table 4. Results from numerical simulation and correlations ($u = 0.5$ m/s)

L [m]	2	4	6	8	10
T_1 [K]	363.15	363.15	363.15	363.15	363.15
T_2 [K]	358.17	353.66	349.73	346.33	343.41
t_1 [K]	288.15	288.15	288.15	288.15	288.15
t_2 [K]	294.54	297.58	301.13	304.09	307.21
ΔP_{it} [Pa]	118.99	224.86	331.11	436.99	542.80
ΔP_{ot} [Pa]	340.28	676.83	1,013.07	1,348.45	1,683.97
U [W/m ² ·K]	983.10	995.67	1,003.65	1,005.83	1,011.93
h_i [W/m ² ·K]	2,953.78	2,954.72	2,954.72	2,954.68	2,957.58
h_o [W/m ² ·K]	2,847.61	2,855.49	2,864.42	2,866.19	2,864.24
ΔP_{Sit} [Pa]	119.95	240.66	361.77	483.34	605.03
Difference [%]	0.81	7.03	9.26	10.61	11.46
ΔP_{Sot} [Pa]	384.48	766.42	1,144.75	1,521.12	1,894.25
Difference [%]	12.99	13.24	13.00	12.81	12.49
U_D [W/m ² ·K]	1,089.83	1,091.51	1,094.65	1,096.93	1,099.88
Difference [%]	10.86	9.63	9.07	9.06	8.69
h_{iS} [W/m ² ·K]	2,811.08	2,792.21	2,777.13	2,763.50	2,752.54
Difference [%]	-4.83	-5.50	-6.01	-6.47	-6.93
h_{oS} [W/m ² ·K]	2,288.93	2,309.87	2,335.14	2,355.90	2,378.15
Difference [%]	-19.62	-19.11	-18.48	-17.80	-16.97

Table 4. Results from numerical simulation and correlations ($u = 0.5$ m/s) (continued)

L [m]	2	4	6	8	10
h_{iL} [W/m ² ·K]	3,044.10	2,934.69	2,883.82	2,850.30	2,826.49
Difference [%]	3.06	-0.68	-2.40	-3.53	-4.43
h_{oL} [W/m ² ·K]	2,227.21	2,254.81	2,287.02	2,313.91	2,342.22
Difference [%]	-21.79	-21.04	-20.16	-19.27	-18.23

Based on the compared results between values from experiment or correlations and simulations, it is confirmed that the model used is appropriate, and the selected parameters of the model are proper also.

From the results, following conclusions are attained:

The heat transfer coefficients difference between the numerical simulations employing k- ϵ model and practical correlations are within 22%, especially for larger lengths the differences are smaller, as shown in Figures 16 and 17.

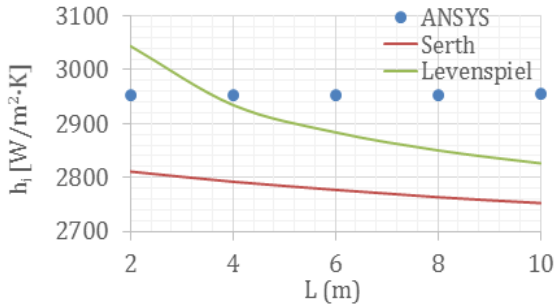


Figure 16. Comparison between practical correlations and numerical simulations for the heat transfer coefficient on hot fluid side

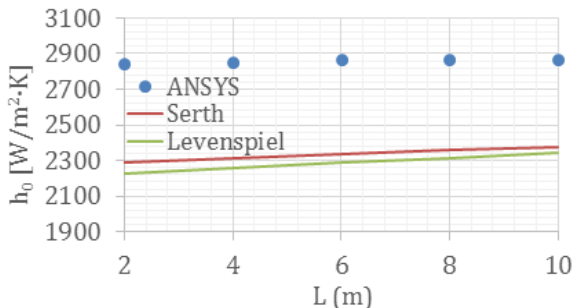


Figure 17. Comparison between practical correlations and numerical simulations for the heat transfer coefficient on cold fluid side

This could be due to the fact that velocity flow profile was not fully developed for low lengths, where a flat velocity profile creates higher gradients than with a fully developed profile, as shown in Figure 18. Figure 19 illustrates a z-velocity contour on y-z planes along z-direction.

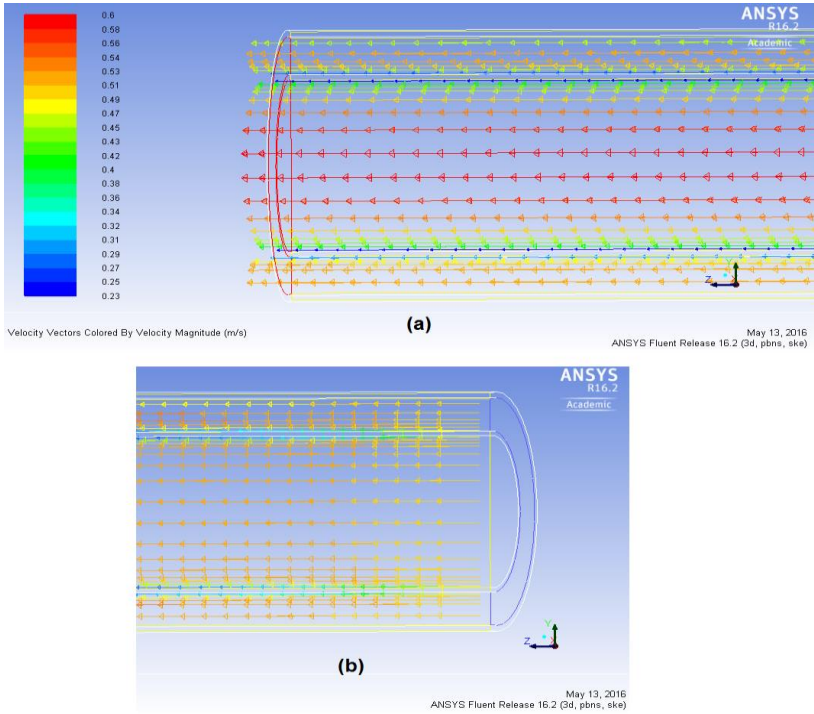


Figure 18. Developed profile at the output (a) and not developed profile at the input (b)

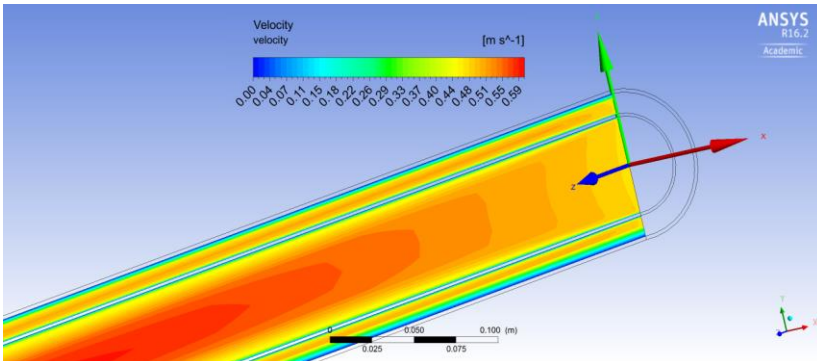


Figure 19. Velocity contour on y-z plane along z-axis

On the other hand, overall heat transfer coefficients calculated have differences below 11%. Typical overall heat transfer coefficients, as shown in Table 5, are given in chapter “Data of Heat Transfer Coefficients” by Walas (1990). The heat transfer coefficient for forced-convection in water are between 10^2 and 10^4 W/(K·m²), according to Levenspiel (1993). Both overall heat transfer coefficients and heat transfer coefficients, compared to simulated results and the correlations employed, are within the range. Therefore, the reliability of heat transfer calculated verified the validity of fluid flow also.

Table. 5. Ranges of overall heat transfer coefficients in double-pipe exchanger

Design U [Btu/°F·ft ² ·h]	Design U [W/K·m ²]
Liquid-liquid media	
50 - 250	284 – 1,419

Figure 20 shows the change of temperature field and temperature distribution in the double pipe at different lengths. According to the flow conditions, the effect of flow condition on the heat transfer and temperature field is observed.

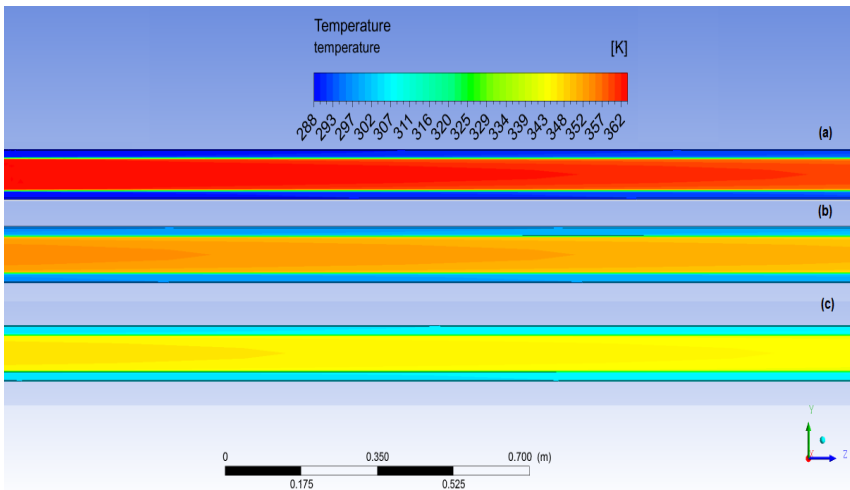


Figure 20. Temperature distribution from 0 to 2 m (a), from 4 to 6 m (b) and from 8 to 10 m (c)

The heat transfer in zones near the wall is higher, as shown in Figure 21, because close to the wall the temperature gradients are higher. The cold fluid increases its temperature along the tube while the temperature in hot fluid decreases.

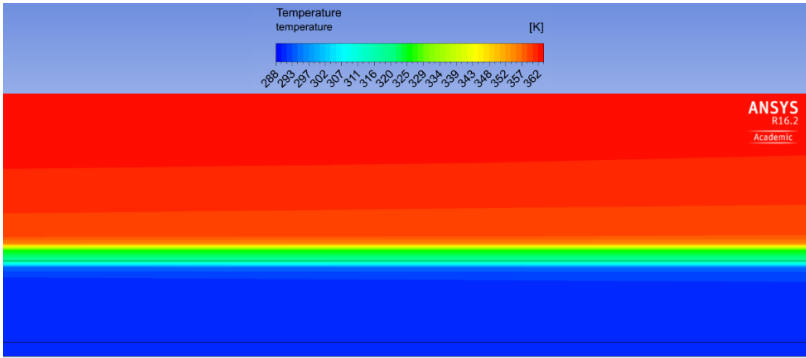


Figure 21. Temperature distribution on the interface

The pressure drop difference between results of the numerical simulations and that of the correlation of Serth (2007) are within 14%. For small lengths, the pressure drop is small too. An increase in the length of tube causes the correlations to deviate more regarding the numerical simulations, as shown in Figure 22.

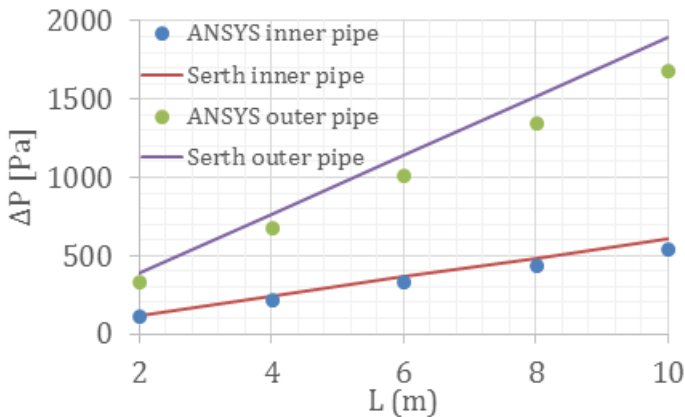


Figure 22. Comparison between practical correlations and numerical simulations for pressure drop

This could be explained due to the complexity of the pressure drop nature. When a tube is used, the roughness has much influence on frictional forces, caused by the resistance to flow. The roughness changes the turbulent profile and, accordingly, this generates pressure drop. However, ANSYS® works with a turbulence model ($k-\epsilon$), which is not part of the concept of “roughness”, so for that turbulence model, the program provides a pressure drop, but in this case the turbulence is not due to the roughness. Figures 23 and 24 illustrate the pressure contours through the double pipe.

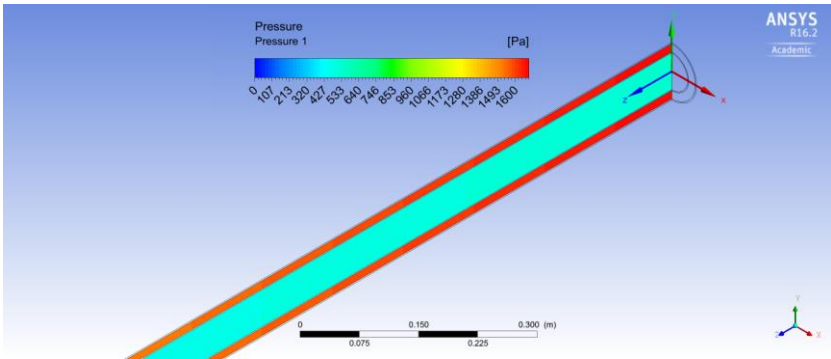


Figure 23. Pressure contours of both fluid at the inlet

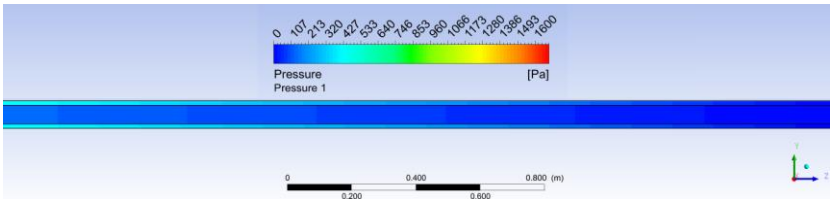


Figure 24. Pressure contours of both fluid at the outlet

It is concluded that the heat transfer model employed is reliable, and reveals characteristics of heat transfer and fluid flow that could not be observed otherwise.

There are several reasons for the differences existing between simulations and correlations. Firstly, engineering correlations used in the project are based on experimental data, not on theoretical solution, where smaller heat exchanger units are used. Secondly, these correlations are made for stabilized profiles. However, ANSYS® Fluent does not work with these profiles in all lengths. Also, some deviation of the results can be attributed to the inability of the computational model to accurately capture film thickness near the wall. Finally, in practice there are many other

components existing besides pipes, such as the effect of the fouling factors on surfaces, joints, etc.

6.2. DOUBLE PIPE HEAT EXCHANGER WITH FINS

Considering the view to increase the performance of the heat exchanger, passive heat transfer augmentation techniques are used. In the present project, double pipe heat exchanger with fins is adopted. It is necessary to make an improved mesh for the smooth double pipe similar to that used in the double pipe with fins. Therefore, the meshing guidelines are similar in both cases to allow their comparison. Meshing section at this point is divided into two blocks:

- Meshing double pipe with fins.
- Improved meshing double pipe - smooth tube.

6.2.1. Geometry

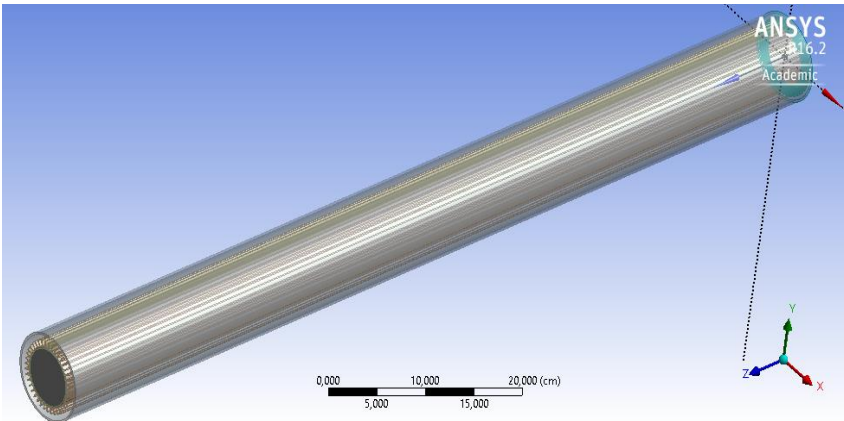


Figure 25. Double pipe with fins geometry

The heat exchanger with inner fins, as shown in Figure 25, is created from four Extrude operations, each of them with depth of 1 meter and referred to a single body like in the geometry of the 1st block. As in the previous block, the inner fluid has been defined with “Add Material” option and the rest bodies with “Add Frozen”. “Add Frozen” option allows to display the independence between bodies, Figure 26.

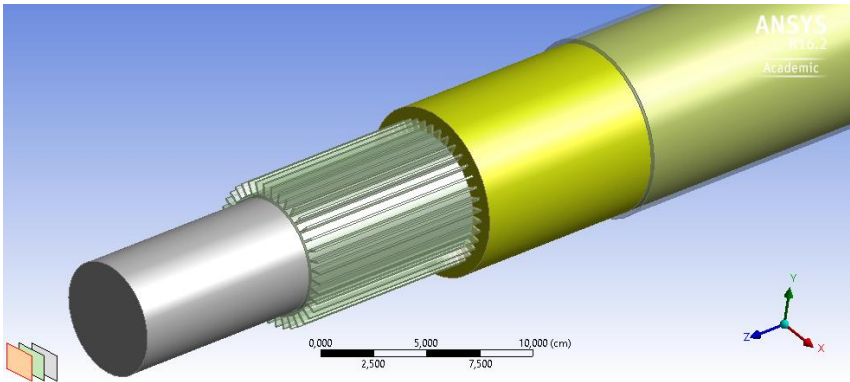


Figure 26. Body sectioned into four parts

The fins are designed from a reference fin. The replicate function is used with a rotation (r) of 18° and a factor (f) of 2.

6.2.2. Mesh

6.2.2.1. Meshing double pipe with fins

There is a clear difference between the current meshing (Figure 27) and the one presented in the previous block (Figure 13). This new mesh causes an increase in the number of nodes and elements: 401,841 and 390,000, respectively. Representation of heat transfer in the finned unit is more complicated, so a more accurate mesh is necessary to reach satisfactory results. Visually, the first difference is the size of the elements, being much smaller than before. This is applied in order to obtain more accurate results in all regions of analysis.

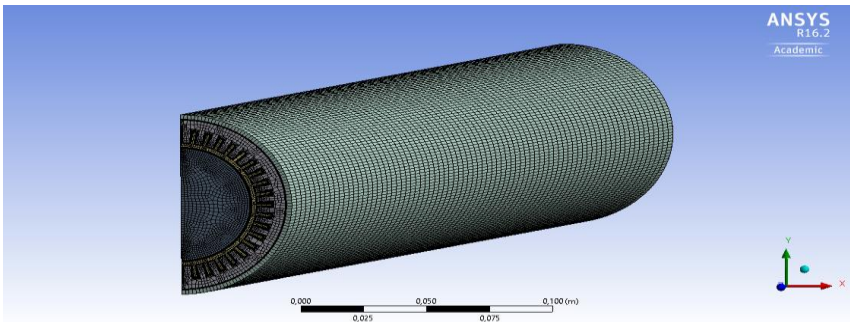


Figure 27. Double pipe finned mesh

The near-wall distribution of the mesh determines the accuracy of the wall shear stress (friction factor) and has an important influence on the development of boundary layers and near wall turbulence structures. For this reason, a selective inflation, as shown in Figure 28, is generated to achieve that the cell density is higher close to the walls to describe more precisely complicated flow fluctuations.

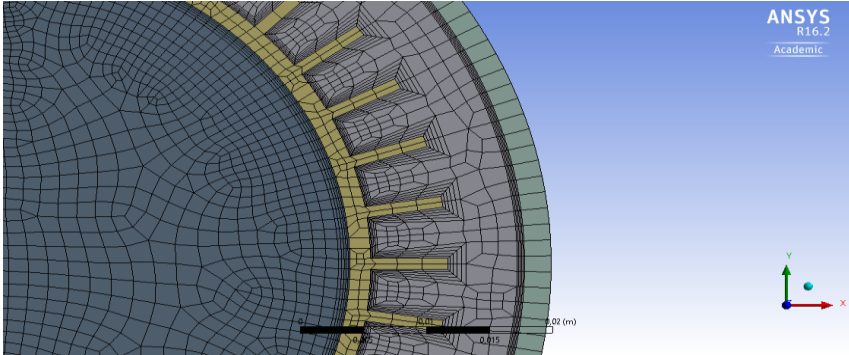


Figure 28. A sector of mesh distribution for front view

Figure 29 shows the typical mesh distribution at the symmetric plane. The model has a fine mesh resolution near the wall and a gradual coarsening of the mesh away from the wall (larger elements in the core region of the pipe). This homogeneous mesh is possible due to the growth factor (BIAS), which allowed to adjust an increasingly fine mesh as the elements approached the walls.

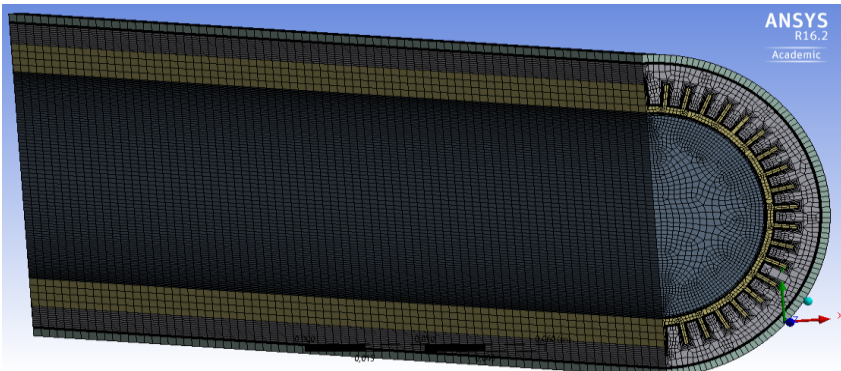


Figure 29. Mesh distribution for symmetry plane

Sectioning geometry at the stage of DesignModeler allows working with simpler geometries and generate a structured mesh step by step. The multizone tool allowed to control the shape of the elements: hexahedral elements are chosen for the inner tube and hexa/prism for the outer fluid. A mesh of hexahedral elements on inner pipe generates this type of elements on that surface, because these elements fit better to the rectangular shape of the fin. Outer fluid is meshed with a hybrid mesh (hexa/prism). The prisms close to the fin give less distortion between elements in these regions. The hexahedral, however, are better in the symmetric region.

The quality parameter such as orthogonal quality and skewness are checked when this block is meshed. Most elements (pink bars, Figure 30) had decent skewness ranges (values of 0-0.5 are ideal).

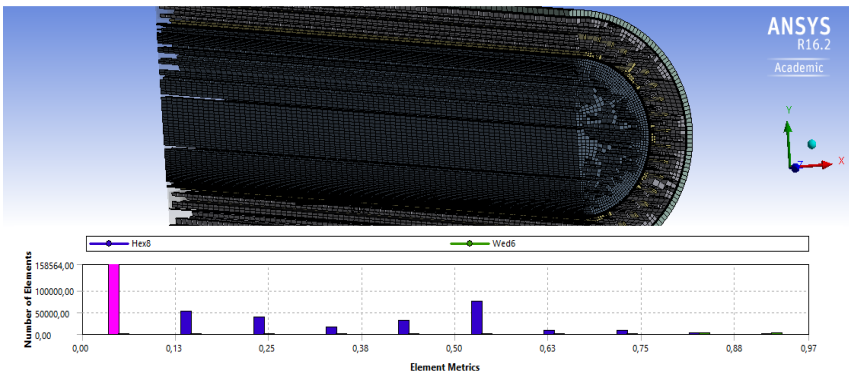


Figure 30. Mesh statistics (skewness) for the double pipe with fins model

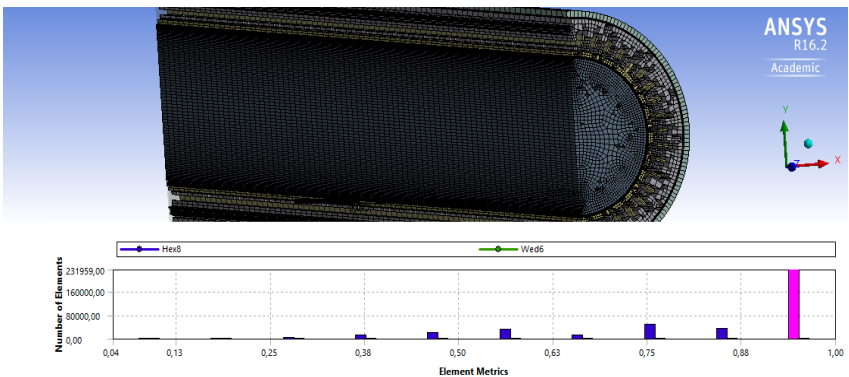


Figure 31. Mesh statistics (orthogonal quality) for the double pipe with fins model

The packaging of the elements is good too, with most orthogonal values between 1 and 0.69, as shown in Figure 31.

6.2.2.2. Improved meshing double smooth pipe

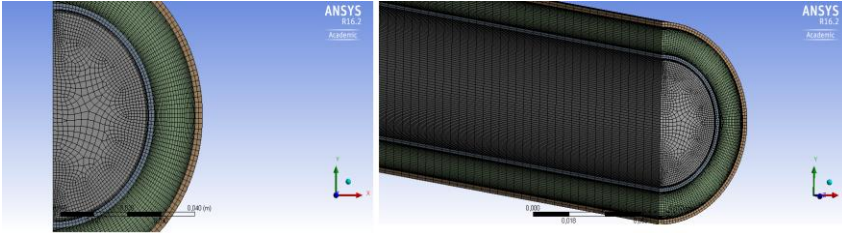


Figure 32. A sector of mesh distribution for front view and side

There is a noticeable change in the mesh, as shown in Figure 32, compared to the Figure 13. Pipe length is reduced to increase the quality of meshing without exceeding the limitation in the number of nodes. This new mesh has 418,284 nodes and 403,360 elements. The same growth factor employed in previous mesh is used for this case, resulting in a structured and uniform mesh, but with a gradual refinement in a region adjacent to the wall to accurately capture the high temperature gradients and local turbulence.

6.2.3. Simulation results of the influence of flow rate and presence of fins

In this second block, the whole analysis is carried out with a mass flow rate of hot water increasing in small increments while the cold water mass flow rate, inlet cold water and hot water temperatures were kept constant. Later, with the same inlet temperatures, fins are used in inner tube to investigate the performance of heat exchanger in terms of increasing the heat transfer by creating turbulence in the fluid flow, the effect of temperature rise and pressure drop in double pipe heat exchanger with the increase in mass flow rate of inner tube fluid as well as to obtain the heat transfer coefficients and the overall heat transfer coefficients. Then, the experimental results are compared with correlations developed for finned tubes, according to Serth (2007). In the Table 6, $h_{i,T,F}$, is the heat transfer coefficient calculated from the correlation Tagle and Ferguson (Serth, 2007), Eq. (18).

The analysis is performed for parallel flow configuration by varying the inner tube side fluid velocity from 0.2 to 0.7 m/s while the outer tube side fluid velocity was kept constant to 0.5 m/s.

The Reynolds number was between 35,000 and 123,000 in hot flow. In Table 6 the experimental and calculated results are compared in both cases: smooth and finned tube.

Table 6. Results from numerical simulation and correlations

(cold fluid data: $u = 0.5$ m/s, $Re = 14,000$ (smooth pipe), $Re = 6,000$ (finned pipe))

u [m/s]	0.2		0.5		0.7	
Re	35,000		87,000		123,000	
	Smooth	Fins	Smooth	Fins	Smooth	Fins
T_1 [K]	363.15	363.15	363.15	363.15	363.15	363.15
T_2 [K]	357.41	357.52	359.72	359.82	360.38	360.47
t_1 [K]	288.15	288.15	288.15	288.15	288.15	288.15
t_2 [K]	289.96	290.59	291.00	291.94	291.41	292.47
ΔP_{it} [Pa]	14.26	14.27	67.72	67.75	122.22	122.19
ΔP_{ot} [Pa]	195.83	512.63	195.83	512.63	195.83	512.64
h_i [W/m ² ·K]	1,226.48	1,523.53	2,628.61	3,258.68	3,521.68	4,366.69
h_o [W/m ² ·K]	3,077.75	2,460.49	3,078.47	2,452.72	3,079.73	2,450.95
U [W/m ² ·K]	881.21	243.15	1,303.44	356.66	1,472.43	401.79
ΔP_{sit} [Pa]	11.61	12.10	60.05	59.36	109.82	106.49
Difference [%]	-18.57	-15.23	-11.34	-12.38	-10.15	-12.84
ΔP_{sot} [Pa]	188.88	554.99	193.33	545.74	195.03	542.34
Difference [%]	-3.55	8.26	-1.27	6.46	-0.41	5.79
U_D [W/m ² ·K]	729.09	248.24	1,045.02	402.36	1,153.60	464.24
Difference [%]	-17.26	2.09	-19.83	12.81	-21.65	15.54
h_{is} [W/m ² ·K]	1,272.25	1,325.14	2,595.06	2,847.78	3,369.06	3,769.38
Difference [%]	3.73	-13.02	-1.28	-12.61	-4.33	-13.68
h_{il} [W/m ² ·K]	1,443.57	1,503.58	2,944.51	3,231.26	3,822.73	4,276.96
Difference [%]	17.70	-1.31	12.02	-0.84	8.55	-2.05
$h_{i,T,F}$ [W/m ² ·K]	1,596.55	1,597.12	3,347.9	3,348.98	4,391.27	4,392.55
Difference [%]	30.17	4.83	27.36	2.77	24.69	0.59
h_{os} [W/m ² ·K]	2,295.25	2,600.40	2,247.71	2,660.58	2,229.74	2,683.55
Difference [%]	-25.42	5.69	-26.99	8.47	-27.60	9.49
h_{ol} [W/m ² ·K]	2,388.92	2,465.90	2,339.44	2,522.97	2,320.74	2,544.75
Difference [%]	-22.38	0.22	-24.01	2.86	-24.64	3.83

Based on the results of the table, following conclusions are obtained:

Figure 33 illustrates the bulk temperature distribution for the cold water along z-profile according to the type of tube. The bulk temperature (represented by points density) in the finned tube is higher than in the smooth one. For each flow velocities in terms of Reynolds from 35,000 to 123,000, as shown in Table. 6, the outlet temperature of the cold fluid in the finned tube is increasing, which increases almost a 1°C compared to the smooth when the velocity is the highest. This could be explained from the phenomenon of turbulence. High velocities of the hot fluid in terms of Reynolds generate a turbulent flow that favors the formation of swirls, helping to transport fluid from one zone to another resulting in a more effective heat transfer.

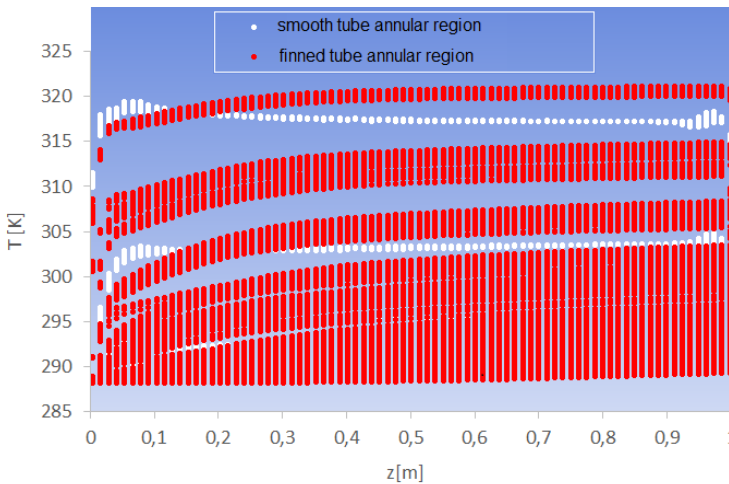


Figure 33. Bulk temperature distribution for the cold water along z-profile

On the other hand, as the Reynolds number increases (as flow rate increases) the hot water flows with high speed and the flow will get less time for the heat exchange process, so the temperature of the hot fluid at the outlet is higher at higher Reynolds. It is concluded that the fins provide an extra surface that improves heat transfer, as shown in Figures 34 and 35. The increase in temperature of cold fluid would be even more significant if the fins had enough time to warm up completely by conduction, since the heat provided by the circulating mass of cold fluid would be even greater. By computational limitations, working with higher tube lengths is not attainable.

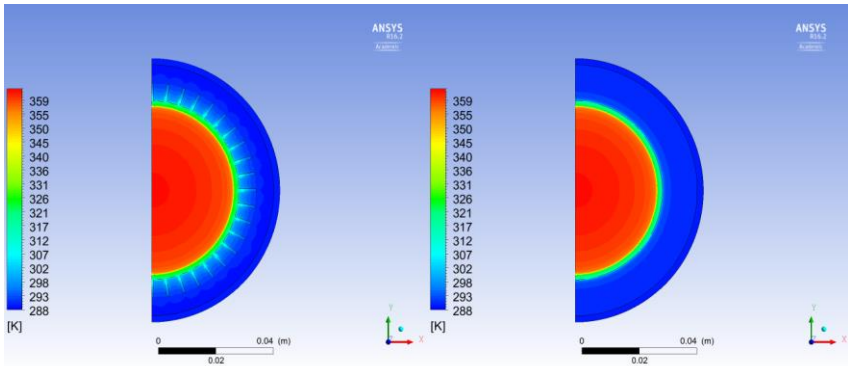


Figure 34. Comparing temperature contour on x-y plane at the outlet

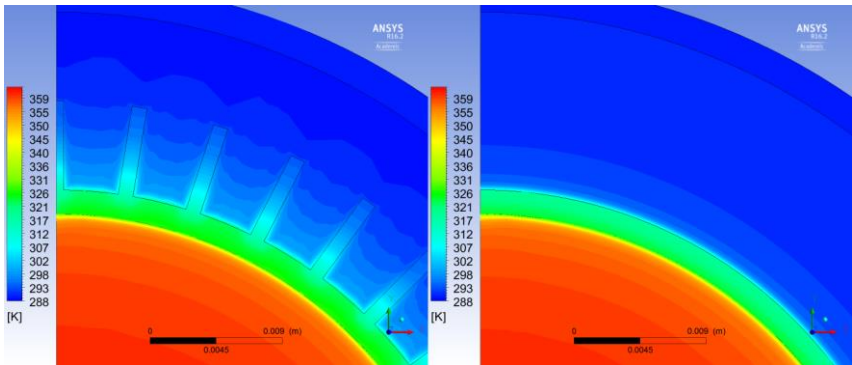


Figure 35. Comparing temperature contour near the interface

As the heat transfer for the finned tube is better, the simulated results of both heat transfer coefficients in this configuration are always higher. It is noted that these are increasing as the Reynolds increases. It is evident from Figure 36 that when the fins are into a plain tube there is a significant improvement in Nusselt number on account of the heat transfer enhancement. This enhancement is partly due to the centrifugal forces resulting from the swirls motion of the fluid with increasing Reynolds and mainly due to the acting of the fins. The heat transfer coefficients on hot fluid side difference between the results obtained through CFD analysis and practical correlations are within 18%. However, the difference between equation from Tagle and Ferguson (Serth, 2007) and numerical results are larger, specifically within 30%. Figure 36 shows that differences between simulated results and the correlations of Serth (2007) are very small for the smooth tubes, nonetheless for the finned tubes these differences are smaller using the

correlations of Levenspiel (1993). Therefore, the obtained results reveal that Nusselt number increases with increasing Reynolds number. The Nusselt number for the finned tube increase up to about 24.1% (or 1.24 times) of the plain tube.

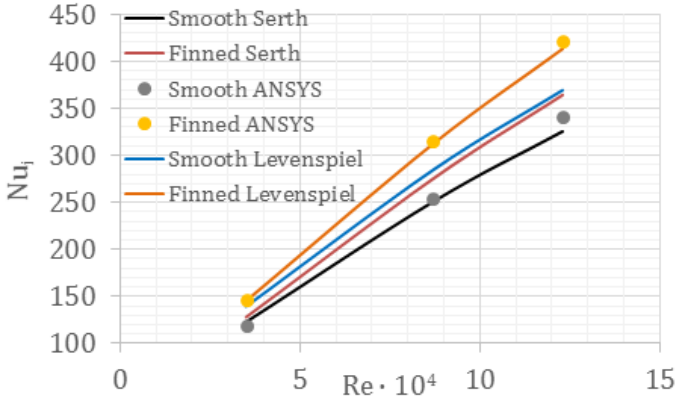


Figure 36. Nusselt number against Reynolds number for different correlations

On the other hand, the heat transfer coefficients on cold fluid side difference between the numerical simulations and correlations for smooth tubes are less than 28%. Note that in the annular region, the differences in magnitude of heat transfer coefficients between simulations results and correlations for finned tubes are less than 10%. This could be for the fact that the fins generate more friction caused by the increased area, resulting in a faster stabilization profile. Figures 37 and 38 show that the velocity profile is more stabilized in the finned tube than in the smooth tube. The correlations are developed for stabilized profiles, hence it makes sense that they have smaller differences in finned tube.

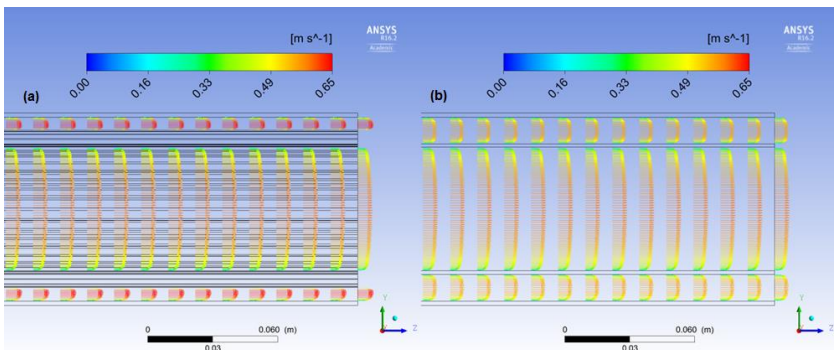


Figure 37. Comparing velocity profiles between double pipe with fins (a) and without them (b)

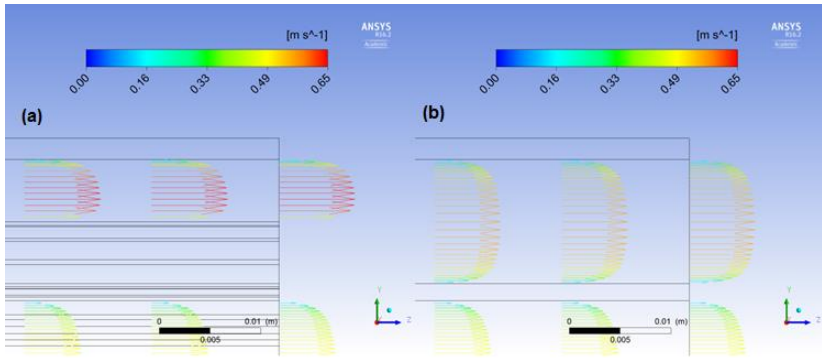


Figure 38. Annular region close up for both cases: tube with fins (a) and smooth tube (b)

The variation of overall heat transfer coefficient with Reynolds for smooth pipe as well as finned pipe is shown in Figure 39. The comparison between overall heat transfer coefficients calculated from the simulations results using Eqs. (7) and (8) and correlations of Serth (2007), indicates a good approximation.

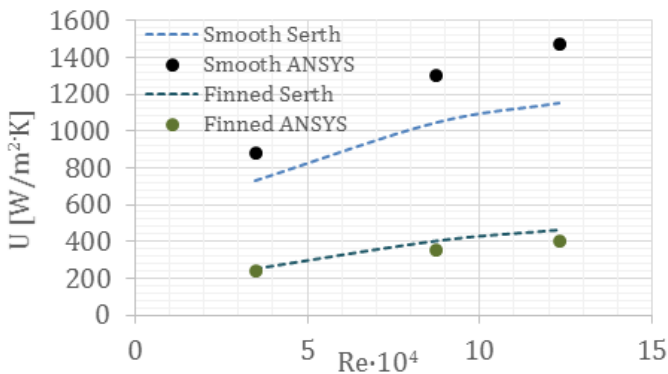


Figure 39. Overall heat transfer coefficients against Reynolds number

The overall heat transfer coefficients are divided by unit area, so it is logical that the coefficients of the finned tube are smaller because the contribution of the surface of the fins (0.53 m^2) compared to the total surface (0.68 m^2) is very large. The smooth tube has a smaller surface, so that gives higher coefficients. The overall heat transfer coefficients increase from 1.51 to 2.65% with increase in Reynolds number as compared to smooth pipe.

Figures 40 and 41 show that the pressure drop in the finned tube is higher. This is because the fins generate more resistance to flow, which contributes to the increase of the pressure drop.

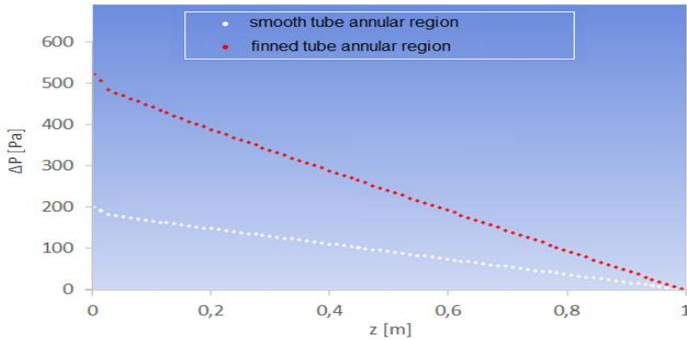


Figure 40. Comparison of pressure drop along z-profile

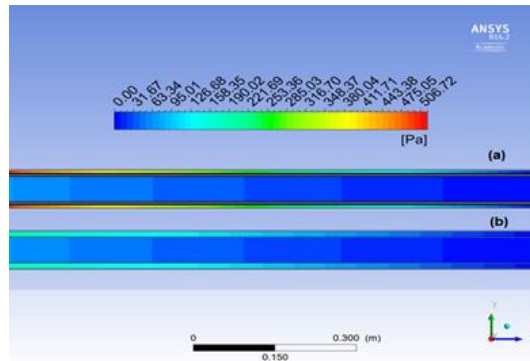


Figure 41. Comparison of pressure contour along z-profile for double pipe with fins (a) and un-finned (b)

Also, the fins reduce the cross sectional flow, therefore to maintain the same flow rate the fluid is accelerated. These high flow velocities, as shown in Figure 42, result in a larger pressure drop across the section of outer pipe. The differences of pressure drop between simulation and correlation are lower than 19%.

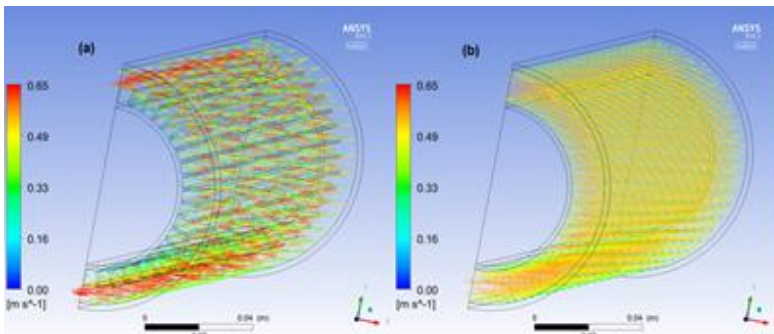


Figure 42. Comparison of velocity vectors along z-profile for double pipe with fins (a) and un-finned (b)

An analysis of friction factor shows that the friction factor gradually is reduced as Reynolds increases. There is a reason that could explain this behavior, with high fluid velocities, that is high Reynolds, the friction with the wall is not so important. The fluid flow is more turbulent and the roughness of the wall have less influence than at low velocities, as shown in Figure 43.

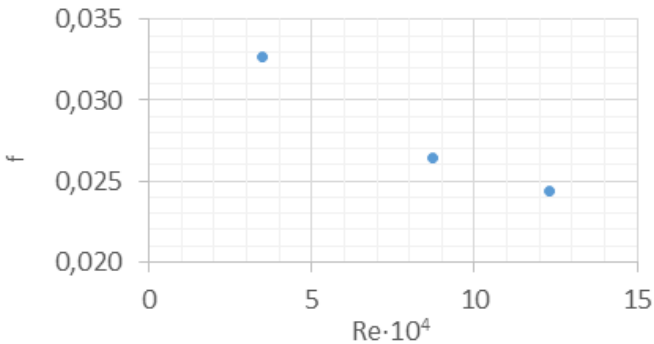


Figure 43. Friction factor against Reynolds number for the inner pipe

As compared to the smooth pipe, the percentage increase in friction factor for the annulus region is about 20.64% (or 1.20 times). Figure 44 shows the variation of pressure drop with friction factor for smooth pipe and finned pipe. Comparing both cases, the pressure drop gradually increases with the increase in friction factor.

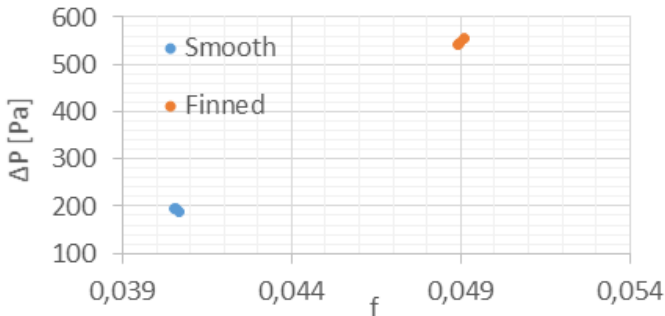


Figure 44. Pressure drop against friction factor for the annulus region

7. CONCLUSIONS

In this project, the simulation results of a double pipe heat exchanger by ANSYS® is in good agreement with practical engineering correlations. The results also show the importance of the fully developed flow profile, being essential to enable accurate measurement when are compared to engineering correlations.

The computation results depend on the quality of the mesh, accordingly meshing plays an important role in CFD analysis, nevertheless a high density of the mesh accompanies a consequential increase in computation time.

The heat transfer in the heat exchanger are improved by using fins. Use of rectangular fins improve the overall heat transfer coefficient significantly with increase in Reynolds number about 2.65%. As Reynolds number increases, the flow causes more turbulence as a result of which heat transfer rate increases, and this enhances Nusselt about 1.24 times (or 24.1%) when compared to the smooth case. On the other hand, when the fins are used, the friction factor obtained is 20.64% higher than the smooth tube. Therefore, the heat transfer enhancement generally accompanies with a penalty of flow resistance elevation when passive heat transfer augmentation methods are used.

It is concluded that ANSYS® is an effective tool for predicting the behaviour and performance in terms of heat transfer and fluid flow processes.

8. REFERENCES

- ANSYS® FLUENT 16.2 in Workbench User's Guide. ANSYS, Inc. License Manager Release 16.2, **2016**.
- Ashby, M.F. *Materials Selection in Mechanical Design*, 4th Edition. Burlington: Elsevier. **2011**, pp 198-201.
- Bejan, A.; Kraus, A. *Heat Transfer Handbook*. Wiley. **2003**, pp 1033-1101.
- Branan, C.R. *Rules of Thumb for Chemical Engineers*. **2005**, pp 29-58.
- Donea, J.; Huerta, A. *Finite Element Methods for Flow Problems*. Wiley. **2003**.
- Eiamsa-ard, S.; Wongcharee, K.; Eiamsa-ard, P.; Thianpong, C. Heat transfer enhancement in a tube using delta-winglet twisted tape inserts. *Applied Thermal Engineering*. **2010**, 30(4), 310-318.
- Ferziger, J.H.; Peric, M. *Computational Methods for Fluid Dynamics*. Springer. **1996**.
- Han, H.; Li, B.; Wu, H.; Shao, W. Multi-objective shape optimization of double pipe heat exchanger with inner corrugated tube using RSM method. *International Journal of Thermal Sciences*. **2015**, 90, 173-186.
- Jaiman, R.K.; Oakley, O. CFD modeling of corrugated flexible pipe. *Proceedings of the International Conference on Offshore Mechanics and Arctic Engineering – OMAE*. **2010**, 6, 661-670.
- Kareem, Z.S.; Abdullah, S.; Lazim, T.M.; Mohd Jaafar, M.N.; Abdul Wahid, A.F. Heat transfer enhancement in three-start spirally corrugated tube: Experimental and numerical study. *Chemical Engineering Science*. **2015**, 134, 746-757.
- Kraus, A.D.; Aziz, A.; Welty, J. *Extended Surface Heat Transfer*. New York: John Wiley & Sons. 2001, pp 443-539.
- Levenspiel, O. *Engineering Flow and Heat Exchange*. Barcelona: Reverté. **1993**, pp 166-170, pp 353-366.
- Lochan, R.; Bashyam, S.; Das, D. Numerical analysis of double pipe heat exchanger using heat transfer augmentation techniques. *International Journal of Plastics Technology*. **2014**, 18(3), 337-348.
- Löhner, R. *Applied CFD Techniques: An Introduction Based on Finite Element Methods*. *International Journal for Numerical Methods in Fluids*. **2002**, 39(1), 97-98.
- McAllister, E.W. *Pipeline Rules of Thumb Handbook*, 7th Edition. Burlington: Elsevier. **2009**, pp 89-120.
- Naphon, P. Heat transfer and pressure drop in the horizontal double pipes with and without twisted tape insert. *International Communications in Heat and Mass Transfer*. **2006**, 33(2), 166-175.
- Patel, K.; Desai, J.; Chauhan, V.; Charnia, S. Evaluation of Hydro Turbine design Computational Fluid Dynamics. November 21-23, **2011**, IIT Madras, Chennai, India. DOI: 10.13140/2.1.3750.3045.
- Perry, R.H.; Green, D.W. *Perry's Chemicals Engineers' Handbook*, 7th Edition. McGraw-Hill: United States of America. **1999**, pp 565-567, pp 1059-1080.
- Peyret, R. *Handbook of Computational Fluid Mechanics*. Academic Press Inc. **1996**.
- Peyret, R.; Taylor, T.D. *Computational Methods for Fluid Flow*. Springer. **1983**.
- Reid, R.C.; Sherwood, T.K.; Prausnitz, J.M. *Properties of Gases and Liquids*. 3rd Edition, McGraw-Hill. **1977**.
- Ruprecht, A.; Heitele, M.; Helmrich, T. Numerical Simulation of a Complete Francis Turbine including unsteady rotor/stator interactions. *Institute for Fluid Mechanics and Hydraulic Machinery University of Stuttgart, Germany*. **2014**.
- Sarada, S.N.; Raju, A.V.S.R.; Radha, K.K.; Sunder, L.S. Enhancement of heat transfer using varying width twisted tape inserts. *International Journal of Engineering, Science and Technology*. **2010**, 2(6), 107-118.
- Serth, R. *Process Heat Transfer: Principles and Applications*. Boston: Elsevier. **2007**, pp 53-56, pp 86-102, pp 127-182, Appendix B: Dimensions of Pipe and Tubing.
- Sinnott, R.; Towler, G. *Chemical Engineering Design*. Barcelona: Reverté. **2012**, pp 816-851, pp 1121-1122.

-
- Stel, H.; Franco, A.; Junqueira, S.L.M.; Erthal, R.H.; Mendes, R.; Gonçalves, M.A.L.; Morales, R.E.M. Turbulent Flow in D-type Corrugated Pipes: Flow Pattern and Friction Factor. *Journal of Fluids Engineering*. **2012**, 134 (12): 121202.
- Walas, S.M. *Chemical Process Equipment Selection and Design*. Newton: Butterworth-Heinemann. **1990**, pp 169-195.

9. ACRONYMS

A	Heat transfer surface area, m ²
A₀	$\pi D_0 L$ = External surface area of inner pipe in a double-pipe heat exchanger, m ²
A_f	Flow area, m ²
A_{fins}	$2n_f N_f b_c L$ = Surface area of all fins in a finned pipe heat exchanger, m ²
A_i	$\pi D_i L$ = Internal surface area of inner pipe in a double-pipe heat exchanger, m ²
A_{prime}	$(\pi D_0 - N_f \tau) n_f L$ = Prime surface area in a finned pipe heat exchanger, m ²
A_{TOT}	Total heat transfer surface area in a finned pipe heat exchanger, m ²
b	Fin height, m
b_c	$b + \tau/2$ = Corrected fin height, m
C_p	Heat capacity at constant pressure, kJ/kg·K
D₀	External diameter of inner pipe in a double pipe heat exchanger, m
D₁	Internal diameter of outer pipe in annulus, m
D₂	External diameter of outer pipe in annulus, m
D_e	Equivalent diameter, m
D_h	Hydraulic diameter, m
D_i	Internal diameter of inner pipe in a double pipe heat exchanger, m
f	Friction factor
G	\dot{m}/A_f = Mass flux, kg/m ² ·s
h₀	Heat transfer coefficient on cold fluid side, W/m ² ·K
h_i	Heat transfer coefficient on hot fluid side, W/m ² ·K
j_H	Modified Colburn factor for heat transfer in the annulus of a double-pipe heat exchanger
k	Thermal conductivity of fluid, W/m·K

k_{pipe}	Thermal conductivity of the pipe, $\text{W/m}\cdot\text{K}$
L	Pipe length, m
m	$(2h_o/(k\tau))^{1/2}$ = Fin parameter, m
\dot{m}	Mass flow rate, kg/s
\dot{m}_c	Mass flow rate for the cold fluid, kg/s
\dot{m}_h	Mass flow rate for the hot fluid, kg/s
N_f	Number of fins on each pipe
n_t	Number of finned pipes
Nu	Nusselt number
P	Pressure, Pa
Pr	Prandtl number
Q	Heat transfer flow on double pipe, kW
r_o	Outside radius of the inner pipe, cm
R_1	Inside radius of the outer pipe, cm
R_2	Outside radius of the outer pipe, cm
Re	Reynolds number
r_i	Inside radius of the inner pipe, cm
s	Specific gravity, lbm/ft^3
T	Temperature, K
t_1	Inlet temperature for the cold fluid, K
T_1	Inlet temperature for the hot fluid, K
t_2	Outlet temperature for the cold fluid, K
T_2	Outlet temperature for the hot fluid, K
T_{ave}	Average temperature of fluid in the annulus of a double pipe heat exchanger, K
t_{ave}	Average temperature of fluid in the inner pipe of a double pipe heat exchanger, K
T_p	Average temperature of prime surface in a finned-pipe heat exchanger, K
T_w	Average pipe wall temperature in an un-finned heat exchanger, K

T_{wt}	Weighted average temperature of finned surface in a finned-pipe heat exchanger,
K	
u	Velocity, m/s
U_D	Design overall heat transfer coefficient, $W/m^2 \cdot K$
VISA	Constant in equation liquid viscosity
VISB	Constant in equation liquid viscosity

GREEK LETTERS

ΔP_f	Pressure drop due to fluid friction in straight sections of pipe, Pa
ΔT_{ml}	Logarithmic mean temperature difference, K
μ	Viscosity, $kg/m \cdot s$
μ_w	Fluid viscosity evaluated at average temperature of pipe wall, $kg/m \cdot s$
η_f	Fin efficiency
η_w	Weighted efficiency
τ	Fin thickness, m

